Vibrational Dynamics of Terminal Acetylenes: I. Comparison of the Intramolecular Vibrational Energy Redistribution Rate of Gases and the Total Relaxation Rate of Dilute Solutions at Room Temperature

Hyun S. Yoo, Merrick J. DeWitt, and Brooks H. Pate*

Department of Chemistry, University of Virginia, McCormick Road, Charlottesville, Virginia 22904

Received: November 23, 2002; In Final Form: October 8, 2003

The population relaxation rate of the first excited state of the acetylenic C−H stretch is compared for room-temperature gas-phase and solution-phase samples of 10 terminal acetylenes. The gas-phase sample pressure is less than 1 atm for all measurements, ensuring that the dynamics occur under collision-free conditions. The relaxation rates are measured using two-color transient absorption picosecond spectroscopy. The population of the excited state is monitored directly through the anharmonically shifted $v = 1-v = 2$ excited-state transition. The relaxation rates of isolated and solvated molecules are strongly correlated and follow a relationship expected for a parallel relaxation process in solution: the total rate in solution is the sum of a molecule-dependent rate related to the isolated molecule dynamics and a molecule-independent solvent-induced relaxation rate. For the terminal acetylenes, the vibrational normal-mode frequencies of the acetylene chromophore and their anharmonic interactions are highly conserved for all terminal acetylenes. Therefore, the observation that a single solvent relaxation contribution to the total relaxation rate describes the solution dynamics for all terminal acetylenes is consistent with the idea that solvent-induced energy relaxation pathways are dominated by the vibrational motions that are in close proximity to the excited state.

Introduction

The flow of vibrational energy within polyatomic molecules plays a central role in chemical kinetics.[1] For example, statistical theories for unimolecular reaction rates, such as the widely used formulation of Rice, Ramsperger, Kassel, and Marcus, assume that the redistribution of vibrational energy is fast compared to the rate of reaction.[2] As a result of its fundamental importance, there has been extensive experimental and theoretical work directed toward understanding the rates and mechanisms of intramolecular vibrational energy redistribution (IVR).[3,4] Experiments have investigated the vibrational dynamics of both isolated, gas-phase molecules and molecules in solution. However, in large part, the fields of vibrational-energy relaxation of isolated and solvated molecules have developed independently.[1,5] This separation can be attributed, in part, to the different experimental techniques commonly used in the two environments: high-resolution, frequency-domain spectroscopy for isolated molecules[4] and time-resolved vibrational spectroscopy for solvated molecules.[6]

The series of papers presented here uses both two-color picosecond infrared spectroscopy and high-resolution molecular-beam spectroscopy to study the vibrational dynamics of a set of 10 molecules in ultracold molecular beams, room-temperature gases, and room-temperature dilute solution. From these measurements, we are able to gain new insight into two important aspects of vibrational dynamics: (1) the relative contributions of the isolated molecule and solvation dynamics to the total vibrational relaxation rate of molecules in solution and (2) the effect of temperature on the isolated-molecule vibrational dynamics. In this first paper, we compare IVR rates of room-temperature gas-phase molecules to room-temperature vibrational-energy relaxation rates in dilute solution (five solvents of the CCl_4 family) measured by ultrafast vibrational spectroscopy. Measuring the population relaxation dynamics of an isolated molecule using the same experimental technique and at the same temperature employed in the solution measurements provides the important baseline time scale of the purely intramolecular dynamics. Knowledge of this rate is necessary to identify the solvent contributions to the relaxation process. The second paper in the series examines the pathway for vibrational relaxation in room-temperature gases and dilute solutions using two-color picosecond transient absorption spectroscopy. The final paper makes a direct comparison between room-temperature and ultracold gas-phase measurements to characterize the thermal enhancements of intramolecular vibrational-energy redistribution rates.

To compare the results for rate measurements of isolated (i.e., gas-phase) and solvated molecules, the vibrational population relaxation mechanisms must be clearly defined. For an isolated molecule, the only process other than slow radiative decay is intramolecular vibrational energy redistribution (IVR).[1,3,4] Coherent excitation of a vibrational normal mode using a broadband laser prepares an initial quantum state where the vibrational motion can be described in a simple manner. In this study, the prepared normal-mode vibration is the acetylenic C−H stretch fundamental. For this normal mode, the motion is localized in a single bond. These modes are sometimes called "local modes" to reflect the localized nature of the initial vibrational motion. In general, this initial state is formed by a superposition of the exact molecular eigenstates, and the initial state undergoes nontrivial time evolution. From the perspective of the molecular eigenstates, this time evolution is a dephasing process. However, to obtain a chemical interpretation, it is more convenient to describe the dynamics using a normal-mode picture. By adopting

* Corresponding author. E-mail: bp2k@virginia.edu.

10.1021/jp027543a CCC: $27.50
Published on Web 01/31/2004

this basis, the subsequent time evolution corresponds to a decay of the population of the initially prepared normal-mode vibrational state. Within this normal-mode picture, the population relaxation can be viewed as energy relaxation in the prepared mode. However, the key feature of IVR is that the total vibrational energy of the molecule is conserved because the energy lost by the prepared vibrational mode must be accepted by the other lower-frequency normal-mode vibrations of the molecule. In this way, the vibrational energy distribution in the normal modes changes, but there is no relaxation of the total energy.

The presence of IVR, but not necessarily the redistribution rate, depends on the molecular size. In the IVR process, the molecule acts as its own "bath" for the energy relaxation of the prepared vibrational mode. Through anharmonic terms in the full molecular Hamiltonian, the localized vibrational energy of the prepared state is redistributed to combination and overtone vibrational states with the same energy. Therefore, the density of vibrational states at the energy of excitation must be sufficiently large to observe an effectively irreversible relaxation. For ultracold molecules in molecular beams, infrared fluorescence dilution measurements demonstrated that extensive population relaxation by IVR requires a threshold vibrational state density of $\sim$10 states/cm^{-1}.[7] Many subsequent studies by high-resolution, molecular-beam infrared spectroscopy have verified this threshold for extensive IVR in molecular beams.[4,8−15] Below this threshold state density, the vibrational normal mode is an approximate eigenstate of the total molecular Hamiltonian, and no redistribution dynamics are observed for the isolated molecule. To this point, there is no systematic study of IVR for room-temperature, gas-phase systems to know whether the extra thermal energy modifies the experimentally observed IVR threshold of ultracold molecules.

In solution, the population of the initially prepared normal-mode vibrational state will decay even if the molecule is too small to show isolated-molecule IVR.[5,6] Here, the solvent can provide the bath for relaxation, and this makes it possible for the total energy of the solute molecule to change. In solution, total energy relaxation can accompany population relaxation. To distinguish between the purely intramolecular and solvent-induced relaxation mechanisms, we refer to the solvent-induced process as vibrational energy relaxation (VER). For a polyatomic molecule, it is unlikely that the VER process relaxes the full energy of the excited state in a single step.[16] Therefore, some of the vibrational energy is retained by the solute but is now found in different normal modes.[17−20] In this sense, there is energy redistribution associated with the VER process. Many previous studies of the vibrational dynamics of molecules in solution have used "small" molecules where the purely intramolecular relaxation process is not expected to occur.[18−23] In these studies, the relaxation dynamics have been called solvent-assisted intramolecular vibrational-energy relaxation (also IVR).[24] In the present study, where results for both "small" (no isolated-molecule IVR) and "large" (isolated-molecule IVR occurs) molecules are presented, we avoid this nomenclature to prevent confusion and reserve the term IVR for the energy redistribution process that would occur even in the absence of solvent.

An important issue in vibrational-energy relaxation is to understand how intramolecular and solvation dynamics interact to determine the relaxation rate and pathway for large molecules in solution.[5,6] For example, the reactivity of a molecule in solution where IVR dominates can be expected to differ significantly from a molecule where VER is fast because in the first case the molecule retains its total vibrational energy. This energy can still be used to overcome barriers to reaction. Current theories of vibrational-energy relaxation of polyatomic molecules in solution are simple extensions of theories for diatomic and small molecules to larger systems. These theories calculate the relaxation rate by assuming that the prepared vibrational mode, such as a hydride stretch, is a stationary state of the molecule.[16,24−30] State-to-state relaxation rates are then calculated by various methods such as time-dependent friction. One conclusion of these studies is that the relaxation rate depends most critically on the interaction with only a few solvent molecules near the excited vibrational mode.[27,30] This result leads to the idea that a molecular-level description of the vibrational relaxation process is possible. However, if the purely intramolecular dynamics dominate, then a very different theoretical approach is required. In this case, the initially localized vibrational motion will rapidly evolve into vibrational motion of all parts of the molecule, and the interaction with several solvent molecules needs to be considered. Furthermore, after the initial redistribution step, the energy in each mode will fluctuate on a time scale governed by the intramolecular dynamics. Theoretical methods that assume a stationary vibrational state will need to be extended to include these dynamics that describe the vibrational dynamics of the "relaxed" molecule.

Several recent studies have started the process of bridging these fields. At the simplest level, the rate determinations for isolated and solvated molecules can be compared directly. For example, it has been noted that there are similar lifetimes for the first excited state of the O−H stretch of some alcohols[31] when measured by high-resolution molecular-beam spectroscopy and time-resolved vibrational spectroscopy in dilute CCl_4 solutions (ethanol: 30−60 ps for the isolated molecule;[32] 13 ps in solution;[33] propargyl alcohol: 30−60 ps (isolated);[34] 14 ps (solution)[35]). In the case of phenol, a direct comparison of time-domain measurements in a molecular beam and dilute solution is possible (14 ps (isolated),[36] 6 ps (solution)[35]). These measurements suggest that the purely intramolecular dynamics make an important contribution to the total relaxation rate of the O−H stretch in solution.

The relative importance of IVR for solution-phase relaxation has also been assessed empirically by measuring the population relaxation rate for a molecule in a series of solvents. For small molecules, where IVR is not expected to be important, the total relaxation rate in solution is often found to be solvent-dependent.[21−23] However, for some molecules solvent-independent relaxation rates are found, and this observation is attributed to the relaxation rate being controlled by fast intramolecular dynamics.[37,38] Another way to investigate the competition between intramolecular and solvent contributions to the relaxation rate is to study the same vibrational mode for a series of progressively larger molecules.[31,37,39−41] Because IVR requires a sufficient density of vibrational states to form a vibrational bath for the relaxation, a transition from solvent-dependent to -independent relaxation rates would be expected. This transition has been observed for the N−O stretch relaxation dynamics for a series of nitro compounds.[38] A related approach is to study the same molecule at different levels of excitation. For a small molecule, IVR may not be operative at the energy of the fundamental but could emerge as an important relaxation pathway for the vibrational overtones. The switch from solvent-dependent to -independent relaxation rates has been recently observed in CH_2I_2, and this changeover has been attributed to a dominant intramolecular-energy relaxation pathway for the overtone.[42−46] For other molecules, solvent-dependent relaxation rates are found for both the fundamental and overtone.[23] These

kinds of indirect studies, however, still fail to answer the important question of whether the observed vibrational-energy relaxation rate in solution matches the isolated-molecule rate in cases where the relaxation is assumed to be under intramolecular control.

One powerful approach to understanding the interplay between IVR and solvent-assisted energy relaxation is the use of supercritical fluids to study the vibrational dynamics in the transition from an isolated to a solvated molecule.[47−50] In the first study of this type on $W(CO)_6$, it has been found that an intramolecular relaxation time scale of about 1 ns is a well-defined limit to the total relaxation rate as the solvent density approaches zero.[48] Furthermore, the same zero-density limit is observed for a series of supercritical fluids.[49] These studies include a time-domain measurement of the relaxation rate of the isolated molecule.[50] One of the time scales in the gas-phase measurement matches the zero-density relaxation rate limit found in the supercritical fluid experiments, and this rate was assigned as the IVR rate on the basis of pressure studies. These experiments suggest that the total relaxation rate in solution has a particularly simple form where the total rate is simply the sum of the IVR rate and a solvent-dependent VER rate. In addition, the results indicate that the IVR rate is maintained at the isolated molecule value when the molecule is solvated.

We have investigated the vibrational dynamics of the acetylenic C−H stretch fundamental for a series of terminal acetylenes (R−C≡C−H) in an effort to understand the contributions that intramolecular and solvation dynamics make to the vibrational relaxation dynamics of polyatomic molecules in solution. Terminal acetylenes provide a few advantages for this kind of systematic study of vibrational-energy relaxation in solution. The acetylenic C−H stretch normal mode involves almost exclusively the movement of a single hydrogen atom in the linear chromophore. The acetylenic chromophore (−C≡C−H) also serves to place the "moving" atom about 3.7 Å away from the rest of the molecule (the R− group). This extension of the hydrogen atom into the solution may help keep the local solvent environment around the acetylenic C−H the same for all terminal acetylenes. Finally, the normal-mode frequencies of vibrational modes that are proximate to the acetylenic C−H stretch (e.g., the C≡C stretch and C≡C−H bend) are nearly constant for all terminal acetylenes. Therefore, if the solvent-induced vibrational-energy relaxation process favors energy transfer to vibrational modes near the excited C−H stretch, then this rate could be expected to be nearly the same for all terminal acetylenes. Readers can refer to Appendix A for more information about spectroscopic features of terminal acetylenes that are important for these vibrational dynamics studies.

Experimental Section

The picosecond infrared spectrometer used in this work is based on an amplified Ti:sapphire laser system (Spectra-Physics, Tsunami Oscillator and Spitfire Amplifier). The system generates picosecond pulses with about 2 mJ of total pulse energy, which is centered around 800 nm, at a repetition rate of 1 kHz. These pulses are split in half to pump two independently tunable optical parametric amplification stages (Quantronix, Light Conversion, TOPAS). The OPA operates with β-barium borate (BBO) crystal to generate two tunable IR pulses (signal and idler). The desired IR frequency for this study is produced through difference frequency mixing of the signal and idler with a $AgGaS_2$ crystal (tunable from 2.5 to 13.5 μm). Infrared pulses of 1.4 ps (25-cm^{-1} bandwidth) with 10−12 μJ of pulse energy are generated in the 3-μm region. We have used the femtosecond laser system, which is nearly identical to the picosecond laser system, to make sure that the picosecond resolution is sufficient for this study and that there are no faster dynamics.

The infrared frequency of one OPA (pump) is tuned to the acetylenic C−H stretch fundamental near 3310 cm^{-1} in solution (∼3330 cm^{-1} for gas-phase terminal acetylenes). The infrared frequency of the second OPA (probe) is adjusted to the vibrational transition frequency of the state to be monitored. For the measurements described in this paper, the probe frequency is tuned to the anharmonically shifted $v = 1-v = 2$ absorption frequency of the acetylenic C−H stretch around 3205 cm^{-1} for solution-phase samples (∼3225 cm^{-1} for gas-phase samples). The maximum time base for the experiment is 600 ps. The full infrared pulse energy (10 μJ) is used for the pump pulse, and only 4% of the probe pulse energy (0.4 μJ) is used. Both pump and probe pulses are focused in the sample by a 100-mm focal length calcium fluoride (CaF_2) lens. A 1-mm-thick CaF_2 sample cell is used for measurements in solutions. The sample is rapidly flowed through the cell using an external pump. For the gas-phase measurements, we have used a static cell, and we have found that a cell length of 2.5 mm provides the highest sensitivity. The transmitted intensity changes are monitored by InSb infrared detectors. The transmitted intensity of the probe pulses are obtained both in the absence of the pump pulse (T_0) and in the presence of the pump pulse (T) to acquire the pump-induced absorption change of the molecules. The measured absorption change at each time delay, $\ln(T_0/T)$, is proportional to the excited-state population. Every other pump pulse is blocked with a synchronized chopper running at 500 Hz so that the values T_0 and T are obtained with two adjacent pulses to minimize the long-time intensity drift of the pump pulse.[51] The relative polarization of the pump and probe pulses is set to the magic angle configuration (54.7°) to suppress the rotational dephasing effect contribution to the measured signal.

Solutions with a concentration of 0.05 M in five solvents (CCl_4, $CHCl_3$, $CDCl_3$, CH_2Cl_2, CCl_3CN) were used at room temperature. On the basis of the intensity of the hydrogen-bonded O−H stretch absorption compared to that of the free O−H stretch of propargyl alcohol in the FTIR spectrum, we estimate that less than 2% of the sample solution is dimers at this concentration. Solution samples were prepared by dissolving molecules in a given solvent except for propyne and butyne, which are gases at room temperature, and they were slowly bubbled into pure solvent. For the gas-phase measurements, the cell volume (12.7 mL) is filled with either the full vapor pressure of the liquid or with a maximum of 1 atm of total pressure for terminal acetylenes that are gases at room temperature. For comparison, the "concentration" of 1 atm of an ideal gas is 0.045 M and is similar to the concentration used in the solution-phase work (0.05 M solutions).

We have used a set of 10 terminal acetylenes to study the vibrational dynamics of room-temperature molecules using picosecond transient absorption spectroscopy. This set includes the molecules with sufficient vapor pressure at room temperature to permit the time-domain measurement of gas-phase molecules. The terminal acetylenes in this study are propyne, propargyl fluoride (PF), propargyl chloride (PCl), 1-butyne (butyne), 3-methyl-1-butyne (methylbutyne), tertbutylacetylene (TBA), 3-fluorobutyne (3FB), 4-fluorobutyne (4FB), methylbutenyne, and trimethylsilylacetylene (TMSA). The structural formulas for these molecules are given in Table 1. Chemicals were purchased from commercial companies, when available, and used without further purification. Some of the terminal acetylene samples (PF, 3FB, and 4FB) were synthesized following

TABLE 1: Lifetimes (ps) of the Relaxation Process in Dilute Solutions at Room Temperature[a]

molecule	CCl_4	$CHCl_3$	$CDCl_3$	CH_2Cl_2	CCl_3CN
H−C≡CCH_3 propyne	22(2.2)	17(1.7)	15(1.5)	17(1.7)	21(2.1)
H−C≡CCH_2F propargyl fluoride	36(3.6)	33(3.3)	32(3.2)	30(3.0)	30(3.0)
H−C≡CCH_2Cl propargyl chloride	51(5.1)	41(4.1)	42(4.2)	34(3.4)	33(3.3)
H−C≡CCH_2CH_3 1-butyne	7.8(0.8)	7.7(0.8)	7.8(0.8)	6.7(0.7)	6.8(0.7)
H−C≡$CC(CH_3)$=CH_2 methylbutenyne	3.6(0.5)	3.9(0.5)	3.3(0.5)	3.6(0.5)	3.7(0.5)
H−C≡$CCH(CH_3)_2$ methylbutyne	5.7(0.6)	5.3(0.5)	5.4(0.5)	5.2(0.5)	4.4(0.5)
H−C≡$CCHFCH_3$ 3-fluorobutyne	13(1.3)	14(1.4)	14(1.4)	14(1.4)	14(1.4)
H−C≡CCH_2CH_2F 4-fluorobutyne	23(2.3)	23(2.3)	19(1.9)	16(1.6)	17(1.7)
H−C≡$CC(CH_3)_3$ *tert*-butylacetylene	5.1(0.5)	4.9(0.5)	4.5(0.5)	4.9(0.5)	4.5(0.5)
H−C≡$CSi(CH_3)_3$ trimethylsilylacetylene	44(4.4)	39(3.9)	30(3.0)	31(3.1)	38(3.8)

[a] Uncertainties are shown in parentheses.

literature methods,[52] and their purities were checked by NMR spectroscopy.

Results

Vibrational-Energy Relaxation Measurements in Dilute Solution. Population lifetimes of the acetylenic C−H stretch in 0.05 M solutions at room temperature are measured using two-color picosecond transient absorption infrared spectroscopy. The population of the first excited state of the acetylenic C−H stretch normal mode is directly monitored through the absorption of the anharmonically shifted (-105 cm^{-1} from the fundamental) $v = 1-v = 2$ vibrational transition. The picosecond transient excited-state absorption spectra can be fit to a single exponential decay expression. All of the measured transient absorption spectra, along with exponential decay fits, are shown in Appendix B. Representative spectra in the other four solvents used in this study are also shown in Appendix B. The relaxation lifetimes in solution obtained from this analysis are listed in Table 1. The errors for the time-domain lifetime measurements reported in Table 1 are determined by the range of values measured in multiple experiments (not the uncertainties in the nonlinear least-squares fit to a single measurement, which are typically much lower).

Intramolecular Vibrational-Energy Redistribution Measurements of Room-Temperature Gas-Phase Molecules. Despite the same effective concentrations in the gas-phase and dilute solution experiments, the change in absorption in the gas-phase experiment is typically a factor of 3 smaller than the corresponding solution measurement. The bandwidth of the excitation laser covers the full rotational contour of the gas-phase absorption. This feature of the experiment differs from the previous work on $W(CO)_6$ where relatively long pulses were used (35 ps) that excited a narrow range of the full gas-phase spectrum.[50] At room temperature, the peak of the rotational distribution occurs at about $J = 30$ for most of the molecules in this study. Coherent excitation excites all of the thermally populated rotational levels. The broadband pulse also prepares several vibrational states through "hot-band" excitation. All thermally populated vibrational levels lie under the excitation profile, with one important exception. The large anharmonic shift of the acetylenic C−H stretch fundamental for vibrational states with the C−H bend excitation (-20-cm^{-1} frequency shift, see Appendix A) ensures that all prepared states monitored in the experiment have no initial excitation in this mode.[53−55]

TABLE 2: IVR Lifetimes and Relative Amplitudes of the Acetylenic C−H Stretch at Room Temperature in the Gas Phase Measured by Probing at a $v = 1-v = 2$ Absorption Frequency[a]

molecule	τ_1(ps)	τ_2(ps)[b]	A_2/A_1	τ_2/τ_1	$\rho^{A1}{}_{3330\ cm^{-1}}$ ($/cm^{-1}$)
H−C≡CCH_3	32(3.2)	520(52)			0.66
H−C≡CCH_2F	89(8.9)				2.3
H−C≡CCH_2Cl	380(70)				4.4
H−C≡CCH_2CH_3	8.3(1.0)	44(4.4)	1.9	5.4	15
H−C≡$CC(CH_3)$=CH_2	4.0(0.6)	23(6.0)	1.5	5.8	36
H−C≡$CCH(CH_3)_2$	5.6(1.0)	25(5.0)	1.5	4.5	460
H−C≡$CCHFCH_3$	22(5.8)	52(14)	0.5	2.3	120
H−C≡CCH_2CH_2F	34(3.4)	140(20)	1.0	4.2	140
H−C≡$CC(CH_3)_3$	5.9(1.0)	39(3.9)	2.2	6.6	700
H−C≡$CSi(CH_3)_3$	96(9.6)				21 000

[a] Uncertainties are shown in parentheses. [b] Three molecules do not require the second time constant for the exponential fit to the decay spectrum, and no τ_2 values are reported for those molecules in the table.

IVR rates of gas-phase molecules are also determined by directly monitoring the excited-state population through the transient absorption signal of the anharmonically shifted $v = 1-2$ vibrational transition absorption. However, the interpretation of gas-phase transient absorption spectra is more complicated than that of the solution-phase spectra. The excited-state population signals for most of the large terminal acetylenes (vibrational-state densities above the empirical molecular-beam IVR threshold of 10 states/cm^{-1}) decay on two time scales. Our analysis (see Appendix C and the following paper) indicates that the initial redistribution process involves population transfer from the first excited state of the acetylenic C−H stretch to vibrational states that include 2 quanta in the acetylenic C−H bend modes. The second, slower process corresponds to full population relaxation to essentially the full local vibrational-state density. In this study, we focus on the initial vibrational-energy redistribution time scale (i.e., the fast component when two redistribution time scales are detected). The initial redistribution rate in room-temperature gases will be shown to correlate with the single relaxation time scale observed in solution. Measured IVR lifetimes are listed in Table 2. The uncertainties in the lifetime determinations reflect the range of values obtained in multiple measurements (not uncertainties in the fit parameters for a single measurement). The vibrational state density at the energy of the first excited acetylenic C−H stretch is also given in Table 2. These values are obtained from a direct harmonic state count using scaled ab initio vibrational frequencies. The density of vibrational states with the same symmetry as the acetylenic C−H stretch is reported. All of the measured gas-phase transient absorption spectra and a detailed analysis of the measurements can be found in Appendix C.

Discussion

To gain insight into the interplay between the IVR dynamics of isolated molecules and the VER dynamics caused by the solvent, we compare the initial relaxation rates in gas and dilute CCl_4 solution in Figure 1. This analysis shows a linear relationship between the total relaxation rate in solution and the initial redistribution rate of isolated molecules. This correlation is consistent with the simple model for population relaxation in solution shown in Figure 2. In this model, the IVR

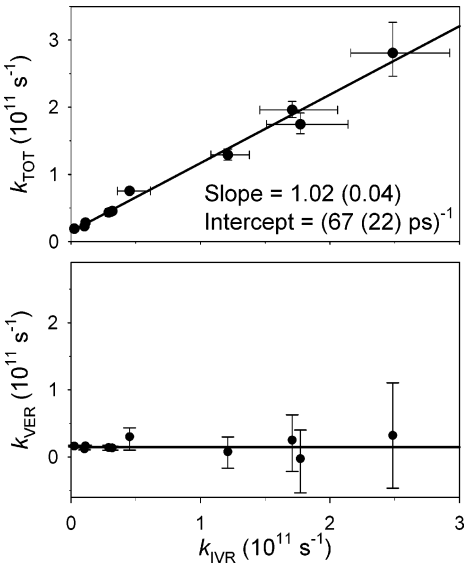

Figure 1. The relationship between the solution rate and IVR rate ($k_{TOT} = k_{IVR} + k_{VER}$) is examined. The linear relationship between the solution and IVR rate indicates that the VER contribution is constant for all terminal acetylenes. The slope of the plot is 1 (1.02(0.04)), implying that the IVR contribution in solution is the same as the gas-phase IVR dynamics. The VER contribution to the total relaxation rate is obtained from the intercept of the linear regression fit ((67(22) ps)$^{-1}$). Calculated VER rates using eq 1 and measured k_{TOT} and k_{IVR} are plotted against the IVR rate in the bottom picture, which shows the constant VER contribution to the total relaxation rate in solution. The uncertainties are determined by the range of values measured in multiple experiments.

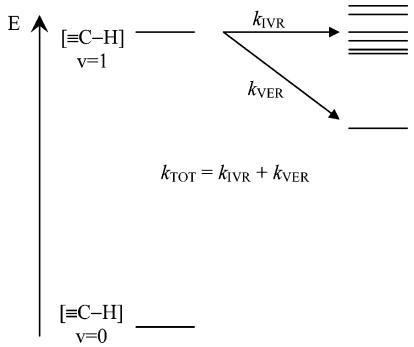

Figure 2. This picture illustrates the simple model for interpreting the total relaxation rate measured in solution. In this model, two competing processes act independently. The final states populated by the intramolecular vibrational-energy redistribution (IVR) pathway are isoenergetic with the initially excited state, and the vibrational-energy relaxation (VER) pathway can transfer population to vibrational states with different energy (most likely lower energy). The total relaxation rate measured in solution is the sum of the molecule-dependent IVR rate and the VER rate.

and VER processes act independently to give the total solution relaxation rate[29] as

$$k_{TOT} = k_{IVR} + k_{VER} \quad (1)$$

where k_{IVR} is the initial intramolecular vibrational redistribution rate and k_{VER} is the solvent-induced vibrational energy relaxation rate.

A linear regression analysis of the data (slope = 1.02(0.04) and intercept = (67 (22) ps)$^{-1}$) points out two key features of the dynamics. The slope determination indicates that the solvent has no effect on the initial IVR rate. The fact that all measurements fall on a single line indicates that a single VER rate describes the solvent contribution to the total relaxation

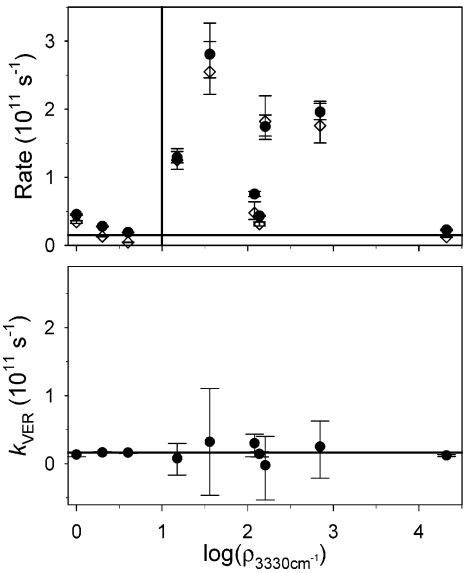

Figure 3. Total relaxation rate in solution (●) and the IVR rate (◇) plotted as a function of the vibrational state density at 3330 cm^{-1}. The rates are not correlated with the vibrational state density of the molecule. The vertical line is the IVR threshold vibrational state density (10 states/cm^{-1}), and the horizontal line indicates the VER rate in CCl_4 solution ((67 ps)$^{-1}$). As this plot illustrates, the solution rate variation is attributed to the molecule-dependent IVR dynamics. In the bottom panel, calculated VER rates using eq 1 and measured k_{TOT} and k_{IVR} are plotted. This plot shows that the solvent contribution to the total relaxation rate in solution is minor compared to the fast IVR contribution. It is also shown in the plot that the VER contribution is constant throughout the series of molecules.

rate in dilute solution for all terminal acetylenes. This latter point is amplified in the bottom panel of Figure 1. In this figure, we assign the VER rate by subtracting the measured IVR rate from the measured total solution rate as suggested by eq 1. Within the measurement uncertainty, a single VER rate is sufficient to describe the solution dynamics of all 10 terminal acetylenes. As discussed above (and more completely in Appendix A), we believe that the observation of a molecule-independent VER rate contribution is related to the constancy of the molecular structure of the acetylenic chromophore (−C≡C−H), the extension it provides to place the moving H atom into solution away from the substituent group (R−), and the constancy of vibrational frequencies and anharmonicities of normal modes associated with the acetylenic structural subunit.[56−58] Many studies of vibrational-energy relaxation in small molecules suggest that the solvent-induced relaxation pathway is dominated by energy transfer to vibrational modes that are in close proximity to the excited mode, especially when there is an anharmonic interaction between them or they contain the motion of the same atoms in their normal-mode descriptions.[17−23,59]

The similarity between the total relaxation rate in solution and the IVR rate is further illustrated in Figure 3. In this figure, the measured solution relaxation rate and the IVR rate are shown as a function of the vibrational state density at 3330 cm^{-1} (given in Table 2). Because we have found that there is a constant VER contribution to the total relaxation rate of the terminal acetylenes in solution, the variation in the observed solution relaxation rates is entirely attributed to the isolated-molecule IVR process. The IVR rates for the terminal acetylenes span a wide dynamic range and are uncorrelated with the total vibrational state density. The combination of these two features produces a distinctive pattern of the relaxation rate when plotted against the vibrational state density. As seen in Figure 3, this

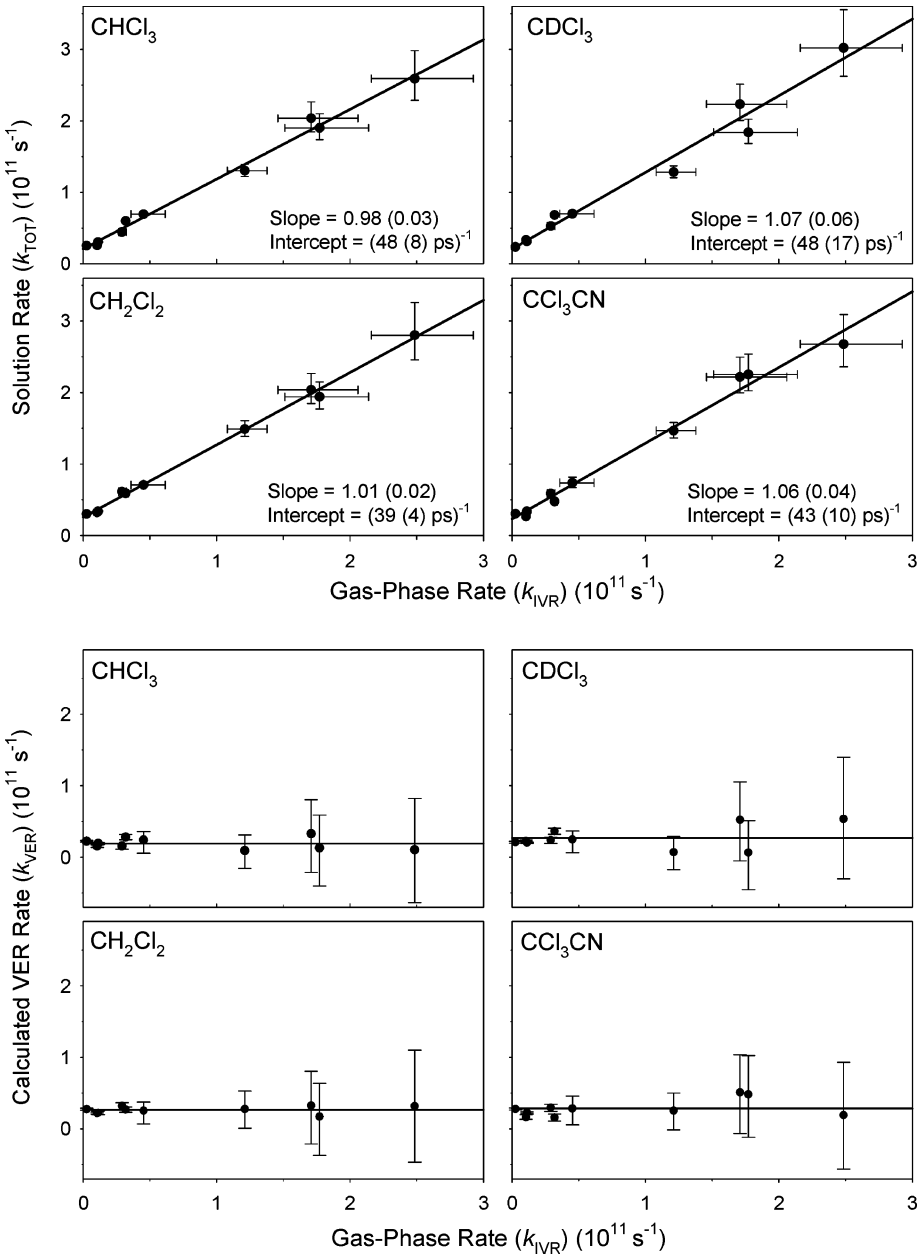

Figure 4. Results of the total relaxation rate measured in four other CCl_4-like solvents. Solution rate (k_{TOT}) is plotted as a function of IVR rate (k_{IVR}). A linear relationship between k_{TOT} and k_{IVR} indicates that the VER contribution to the total relaxation rate is constant for all of the solvents. These results show that gas-phase IVR dynamics survive the transition to solution in all cases (slope = 1). The VER rate is solvent-dependent, as shown by the variation in the intercept of the linear regression line. In the bottom half of the figure, calculated VER rates are plotted as a function of IVR rates to show that the solvent-induced rates are constant for all of the molecules in a given solvent and also minor compared to fast IVR rates.

pattern is preserved in the solution rates. The IVR threshold for ultracold molecules determined from molecular-beam experiments (~10 states/cm^{-1}) is indicated by the vertical line in Figure 3. The onset of fast initial IVR rates in room-temperature gases appears to respect the ultracold-molecule threshold. Also shown in Figure 3 are the calculated VER rates plotted as a function of the vibrational state density at 3330 cm^{-1}. This plot emphasizes the fact that the VER rate is independent of the total vibrational state density (and, in fact, any details of the structure of the substituent group). This result also supports the idea that the solvent-induced relaxation of the acetylenic C−H stretch involves the vibrational modes of the chromophore. We also note that the solvent rate contribution is slow (lifetime of 67 ps). For almost all large terminal acetylenes (molecules above the "IVR threshold"), the total relaxation rate in solution is dominated by the purely intramolecular dynamics.

To test the generality of the simple rate model, the total relaxation rate has been measured in four more CCl_4-like solvents, and eq 1 has been found to hold. The measurement results are displayed in Figures 4 and 5 (equivalent to Figures 2 and 3). The VER rates in the different solvents are characterized by a relaxation lifetime and shown for each solvent in Figure 4. As was the case for CCl_4, the slope of the linear relationship is one (within the linear least-squares fit uncertainty) showing that the purely intramolecular relaxation rate is not modified by solvent. Also, within our measurement uncertainties, a single VER rate contribution can be used to describe the solution dynamics of all 10 acetylenes. This VER rate is solvent-

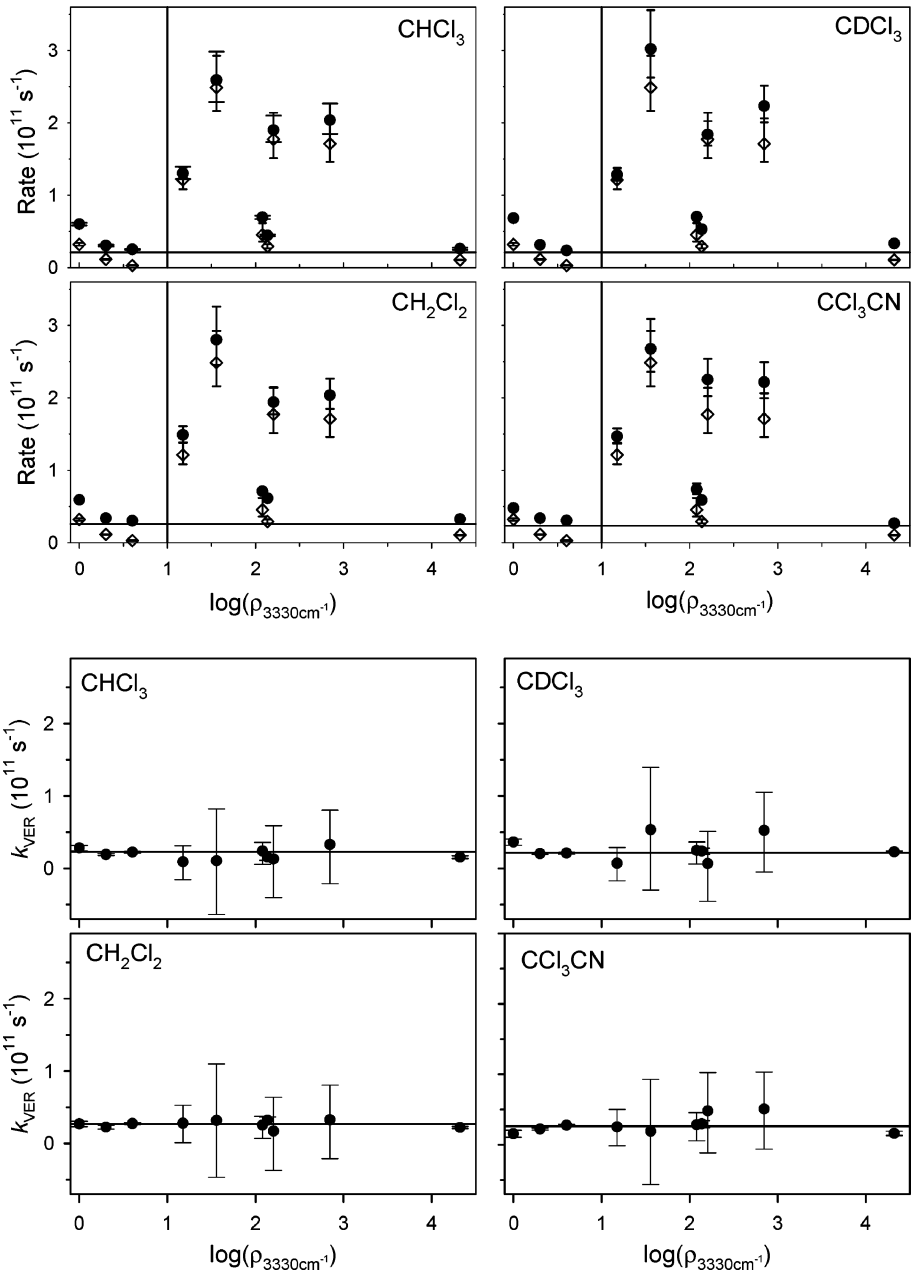

Figure 5. Total relaxation rate in solution (●) and the IVR rate (◊) plotted as a function of the vibrational state density at 3330 cm^{-1}. The IVR threshold vibrational state density (10 states/cm^{-1}) is shown as a vertical line, and the horizontal line indicates the VER rate in each solvent (Figure 4). The solution rate variation follows almost exactly the change in the IVR rate. Also, the difference between the IVR rate and the solution rate is small and almost the same for each molecule, which implies that the solvent-induced VER rates are constant throughout the series of molecules. These effects are shown in the bottom half of the figure, where calculated VER rates using eq 1 and measured k_{TOT} and k_{IVR} are plotted as a function of the vibrational state density at 3330 cm^{-1}.

dependent (lifetimes of 39−67 ps), as expected, but remains slow compared to the intramolecular dynamics for most of the terminal acetylenes.

Finally, the analysis presented above has focused on a rate comparison. When only rates are considered, we find that the intramolecular vibrational-energy redistribution rate of the collision-free molecules is unchanged by solvation. However, the solvent does influence the dynamics by increasing the extent of the population relaxation produced by this initial IVR process. For the gas-phase molecule, this initial redistribution process removes only about 30−50% of the population from the excited state. However, in solution the population relaxation is complete (as indicated by the observation of a single-exponential decay). In Appendix C, we show that the gas-phase measurements are consistent with a hierarchical IVR process involving a sparse set of vibrational levels in the first tier. Incomplete population decay resulting from IVR into this tier is caused by quantum mechanical interference effects of the amplitude returning from the first-tier states to the acetylenic C−H stretch. In a future publication, we will show that when pure dephasing effects of the solvent are added to the tier model the initial population decay becomes complete but maintains the initial rate observed in the partial population decay of the original tier model.

Conclusions

The IVR dynamics of room-temperature gas-phase samples of the terminal acetylenes have been investigated using picosecond pump−probe spectroscopy. This measurement technique has allowed us to investigate the vibrational dynamics of

collision-free and solvated molecules with the same technique and at the same temperature. The experiments show that the IVR dynamics of the acetylenic C−H stretch for most of the molecules in our study occur on two distinct time scales. This behavior is examined in more detail in the next paper of this series where we describe the pathway for IVR and how it is affected by solvation.

Using the initial IVR rates for the room-temperature gas-phase samples, the simple model for the total relaxation rate in solution (Figure 2, eq 1) is found to work extremely well. For the terminal acetylenes, the total relaxation rate in solution is well described by the sum of a molecule-dependent IVR rate and a solution VER rate that is approximately the same for all terminal acetylenes. The IVR contribution to the total solution relaxation rate is the same as the collision-free IVR rate, showing that the IVR dynamics are the same in the isolated and solvated molecule. This behavior is, perhaps, not unexpected because many studies have shown that intramolecular anharmonicities are the same for gas- and solution-phase systems.[60−62] Because the anharmonic interactions cause IVR in the isolated molecule, the initial relaxation rate can be expected to remain the same in solution.

With the exception of propargyl chloride, the initial IVR rate for all of the terminal acetylenes is comparable to, or much faster than, the VER contributions of the CCl_4-like solvents included in this study. A theoretical description of solvent energy relaxation for these molecules would, therefore, need to include the intramolecular dynamics.[29] For example, the initial IVR process occurs before the solvent can relax the energy of the acetylenic C−H stretch for many of the molecules in this study. In this case, the solvent-induced energy relaxation dynamics involve interactions with a molecule where the vibrational energy fluctuates through the vibrational modes under the control of the intramolecular vibrational-energy redistribution dynamics. The extension of current theories, which assume the preparation of a stationary state of the molecular Hamiltonian,[16,24,26−30,63−65] to include the intramolecular dynamics presents an important new challenge to the field of vibrational-energy relaxation.

Acknowledgment. We thank Ted Heilweil for his generous assistance during the development of the picosecond transient absorption spectrometer. We thank John Keske and Frances Rees for their help with the terminal acetylene sample set. We also thank Sergei Egorov, Martin Gruebele, David Leitner, and Ned Sibert for discussions of the connection between the isolated molecule and solution-phase relaxation rates. This work was supported by the Chemistry Division of the National Science Foundation (CHE-0078825) and the Optical Sciences and Engineering Division of the National Science Foundation. Additional support for this work came from the SELIM Program and the AEP Program at the University of Virginia.

Appendix A: Vibrational Spectroscopy of the Terminal Acetylenes

In this section, we describe some common features of the vibrational spectroscopy of terminal acetylenes that are important in the interpretation of the time-domain spectra. The acetylenic functional group, −C≡C−H, is an ideal vibrational chromophore. Three of the normal-mode frequencies of this group are highly conserved in all compounds: the acetylenic C−H stretch (3330 cm^{-1}), the acetylenic C≡C stretch (2000 cm^{-1}), and the in-plane acetylenic C−H bend frequencies (630 cm^{-1}).[57,58] For most molecules, the out-of-plane acetylenic C−H bend has the same frequency as the in-plane bend. However, in special cases, most notably, in molecules where a double bond is in conjugation with the acetylenic bond, this frequency is lowered relative to the in-plane normal mode.[57] The frequencies of the two R−C≡C bend normal modes (i.e., the acetylene wags) vary with the structure of the R group because of the mass differences of the substituent. In all cases, these are low-frequency modes with observed frequencies in the range of 150−300 cm^{-1}. In dilute solution, the frequency shift for each normal mode associated with the chromophore is the same for all terminal acetylenes.

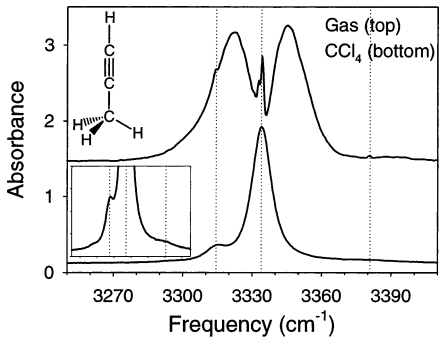

Figure A1. FTIR spectra of propyne in gas-phase (top) and in CCl_4 solution (bottom) shown for the acetylenic C−H stretch region. There is a large anharmonic interaction between the acetylenic C−H stretch and the acetylenic C−H bend. The acetylenic C−H stretch fundamental frequency shifts about −20 cm^{-1} when 1 quantum of the C−H bend is excited because of the interaction. There also exists a strong intramolecular perturbation between the first excited state of the acetylenic C−H stretch and the vibrational combination band of the acetylenic C≡C stretch + 2 C−H bend, leading to a weak perturbation observed at higher frequency. Vertical reference lines indicate the frequency positions of the acetylenic C−H stretch fundamental (3335 cm^{-1}), the hot band with 1 quantum of the C−H bend excited (3315 cm^{-1}), and the combination band of the C≡C stretch + 2C−H bend (3380 cm^{-1}) for gas-phase propyne. The FTIR spectrum of propyne in dilute CCl_4 solution is linearly shifted about +20 cm^{-1} to match the gas-phase positions. The solution spectrum shows that the gas-phase anharmonicities are preserved in solution.

The anharmonic constants of the vibrational modes associated with the chromophore are also conserved for the family of terminal acetylenes. The diagonal anharmonicities (x_{ii}) of the acetylenic C−H stretch and C−H bend can be determined from the shift of the first overtone frequency and are about −53 and −11 cm^{-1}, respectively. A few off-diagonal anharmonicities (x_{ij}) can be determined from the infrared spectrum. The room-temperature FTIR spectrum in the region of the acetylenic C−H stretch of propyne in the gas phase is shown in Figure A1 to illustrate these values. The spectrum of propyne in dilute CCl_4 solution is also shown for comparison. There is a large anharmonic interaction between the acetylenic C−H stretch and the C−H bend.[53−55] This interaction shifts the fundamental absorption frequency of the C−H stretch by −20 cm^{-1} for each quantum of C−H bend. The vibrational hot band from the thermally populated C−H bend fundamentals is observed in all terminal acetylenes and has about 10% of the intensity of the main band at room temperature.[53] The acetylenic wag is the only other vibrational mode that gives an observable shift of the fundamental frequency in the low-resolution FTIR spectrum.[54] The anharmonic interaction of these modes with the C−H stretch leads to a much smaller shift of the C−H stretch fundamental than the C−H bend, typically about 1 cm^{-1} for each quantum of wag excitation. Because this normal mode has a low frequency, a hot-band progression is observed in the spectrum. A similar progression for this mode can be observed

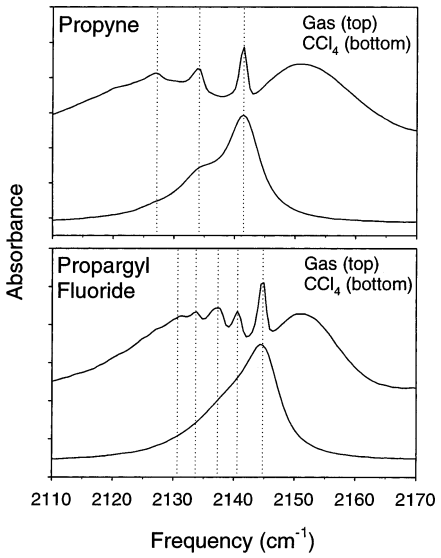

Figure A2. FTIR spectra of propyne and propargyl fluoride shown for the acetylenic C≡C stretch region. There is an anharmonic interaction between the C≡C stretch and the acetylenic wag. The gas-phase sequence band structure, caused by thermal population of the R−C≡C wag, is observed for both molecules. The frequency separation between adjacent hot-band Q branches is ∼7.7 cm^{-1} for propyne and ∼4.3 cm^{-1} for propargyl fluoride. The sequence band structure persists in dilute CCl_4 solution as shown. The solution spectra are shifted by +11 cm^{-1} (propyne) and +9 cm^{-1} (propargyl fluoride) to match the gas-phase frequencies.

for the C≡C stretch (Figure A2) with a stronger anharmonic shift of about −5 cm^{-1}. The anharmonic interactions of the C−H stretch and C−H bend and the C≡C stretch and acetylene wag are also observed in dilute solution with the anharmonic constants unchanged.

The last important feature of the vibrational spectroscopy of terminal acetylenes is the presence of a strong intramolecular perturbation between the first excited state of the C−H stretch and the vibrational combination band: C≡C stretch + 2C−H bend.[11,66] This interaction is similar to the strong stretch−bend interactions known for aliphatic C−H stretches that have interaction matrix elements of about 70 cm^{-1}.[3] For the acetylenes, there is a significant lowering of the bend frequency that keeps the usual stretch−bend interaction out of resonance. However, the energy difference between the C−H stretch and C−H bend overtone almost exactly matches the frequency of the C≡C stretch. This same perturbation is known in acetylene (C_2H_2), where it is essentially degenerate.[67] For most terminal acetylenes, the zeroth-order states are out of resonance by 30−50 cm^{-1}, leading to a weak perturbation in the spectrum. This perturber is observed at ∼3380 cm^{-1} in gas-phase propyne[11,66] (Figure A1) and is also observed in dilute CCl_4 solution. The solvent shift of the combination band is found to be about the same as the C−H stretch excited state so that the same extent of vibrational state mixing is observed in the solution- and gas-phase spectra. Using the molecular-beam spectrometer, we have observed the weak band in butyne (3370 cm^{-1}) and tertbutylacetylene (3364 cm^{-1}).[68] The interaction matrix elements can be determined by a two-state perturbation and have an interaction matrix element of about 5−8 cm^{-1}. This perturbation can be tuned to almost exact resonance when the acetylene is placed in conjugation with a carbon double bond (e.g., methylbutenyne).

The existence of this off-resonance interaction[69,70] means that the nomenclature of the vibrational state being prepared in the experiment must be carefully considered. The interaction between the acetylenic C−H stretch and the C≡C stretch + 2C−H bend combination band produces two vibrationally mixed quantum states separated in energy by 30−50 cm^{-1}. One of these quantum states has the dominant character of the C−H stretch (∼95%) and is typically called the "C−H stretch" despite the fact that wave function contains a small contribution from the coupled combination band. Preparation of the acetylenic C−H stretch normal mode would require coherent excitation of both of these mixed quantum states. However, when picosecond excitation is used to prepare the initial vibrational state, the bandwidth of the laser will excite only the mixed state with a dominant C−H stretch contribution. Although it lacks precision, this prepared state will be called the "acetylenic C−H stretch" in the papers of this series.

The terminal acetylenes also offer a few minor advantages for a longitudinal study of vibrational-energy relaxation. Ab initio calculations show that the acetylenic C−H stretch normal mode consists almost entirely of the motion of the hydrogen atom for all terminal acetylenes.[71] The displacements of the first and second carbon atoms are factors of 8 and 30 smaller than the hydrogen motion, respectively, and there is essentially no motion of atoms in the substituent group (R). Therefore, the same local-mode motion is prepared by coherent vibrational excitation for all molecules. Furthermore, the linear chromophore structure extends the excited hydrogen atom motion about 3.7 Å away from the substituent group. Therefore, the local solvation environment of the acetylenic hydrogen can be expected to be independent of the geometry of the substituent.

The C−H stretch fundamental frequency is ∼3330 cm^{-1} and is well separated from other hydride stretch frequencies. This places the transition into a spectral window that is relatively clean even for solvents containing aliphatic C−H stretches (e.g., $HCCl_3$). The C−H stretch intensity is about a factor of 2 higher than any other hydride stretch, leading to high sensitivity. Many of the compounds in this study are simple hydrocarbons with low boiling points that permit time-domain studies of room-temperature gas-phase samples. Acetylene is a common functional group that can be manipulated by simple synthetic techniques, making it possible to tailor the molecules for important physical or spectroscopic features.

Appendix B: Solution-Phase Data Analysis

Two-color measurements have been used to measure the total relaxation rate of solution-phase terminal acetylenes to avoid the problems caused by the anharmonic shifting of the fundamental frequency during the relaxation process. All of the relaxation signals are fit to a single-exponential decay expression, except for methylbutenyne, as shown in Figures A3 and A4. The unique intramolecular dynamics of methylbutenyne (Appendix C) cause the excited-state absorption signal to decay biexponentially in solution. Femtosecond measurements of methylbutenyne in CCl_4 show that the fast time scale is 0.6 ps, which cannot be properly resolved with the picosecond system, and the slower time scale is about 3.6 ps, which matches the time scale of the single-exponential decay fit to the picosecond measurements. The unusual dynamics of methylbutenyne will be analyzed in a future publication.[72] Residuals of the single-exponential fit to the transient absorption spectra are also shown in Figures A3 and A4 to show the quality of the fits.

The pump laser efficiently excites all thermally populated vibrational states within the 25-cm^{-1} bandwidth of the laser. This bandwidth includes all thermally populated vibrational states except states with excitation in the acetylenic C−H bend

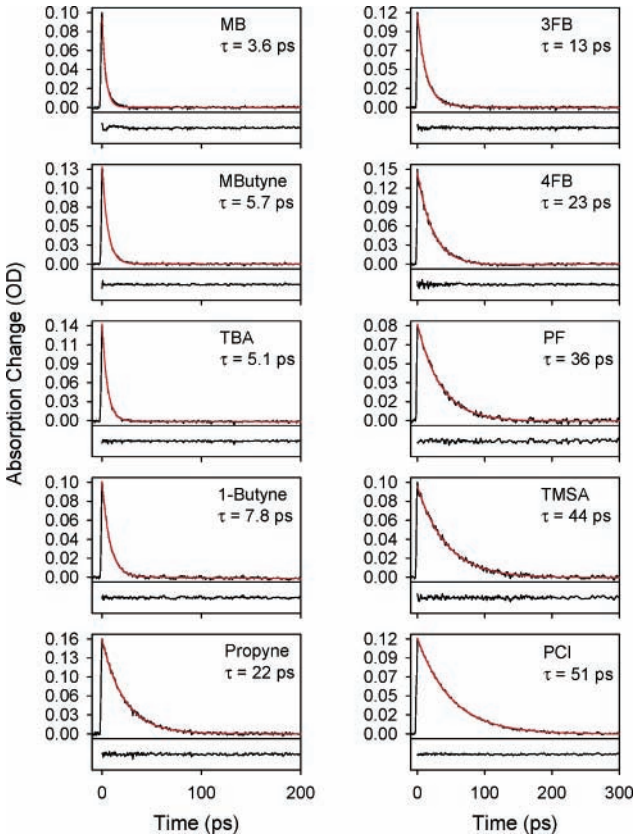

Figure A3. Transient absorption spectra (measured at the $v = 1-v = 2$ transition frequency) of 10 terminal acetylenes in dilute CCl_4 solutions. Corresponding decay lifetimes are included in the plots. The decay of the excited-state absorption signal is fit to a simple single-exponential decay expression as shown (red line). Methylbutenyne displays a unique behavior that will be explored in a future publication.[72] Also shown are the residual plots of each single-exponential fit to the transient absorption signal.

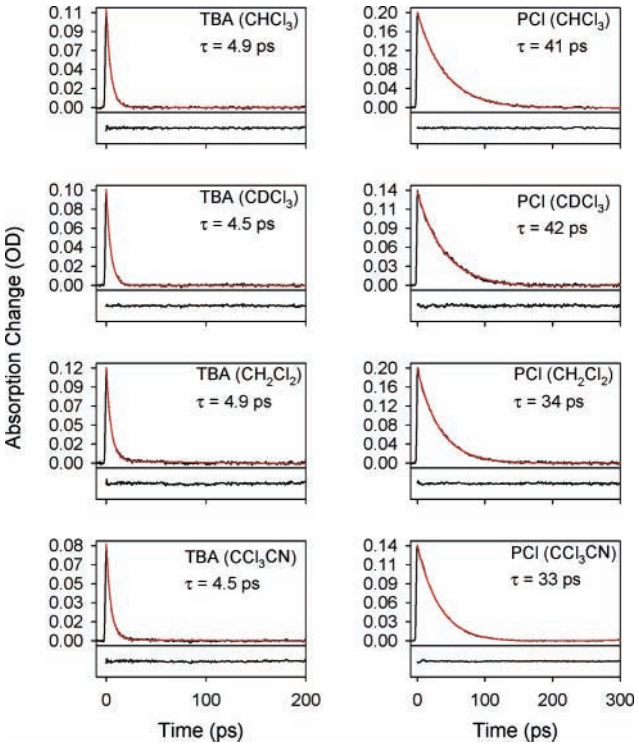

Figure A4. Transient absorption spectra of TBA (fast IVR) and PCl (no IVR) in other CCl_4-like solvents along with their lifetimes. The decay of the excited-state population is a simple single exponential in all of the solvents, and a single-exponential fit to each spectrum is shown (red line). Residual plots of each single-exponential fit to the transient absorption signal are also shown.

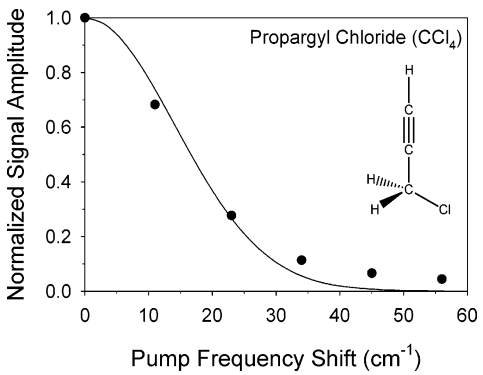

Figure A5. Efficiency of off-resonance excitation examined with propargyl chloride in dilute CCl_4 solution. The pump frequency is tuned to the blue from the acetylenic C−H stretch fundamental, and the relative amplitude of the induced absorption at $t = 0$ is monitored as a function of the pump frequency shift. Filled circles indicate the measured amplitude at each pump frequency shift. A simple calculation of the overlap between the frequency bandwidth of the pump pulse and the solution-phase line shape reproduces the signal amplitude well, as shown by a solid line.

where the anharmonicity constant is very large (20 cm^{-1}). Despite being off-resonance, it is still possible to excite these hot-band transitions in the picosecond experiment. The vibrational dynamics of the combination state produced by the off-resonance excitation of the hot band could be different, especially considering the strong anharmonic interaction between the acetylenic C−H stretch and C−H bend. We have examined the efficiency of off-resonance excitation by tuning the pump laser to higher frequency from the main acetylenic C−H stretch absorption feature of propargyl chloride while maintaining the probe laser at the $v = 1-v = 2$ transition frequency. The relative amplitude of the induced absorption at $t = 0$ as a function of the pump frequency shift is shown in Figure A5. The relaxation lifetime remains constant as the laser is shifted to higher frequency. The signal amplitude is well reproduced by a simple calculation of the overlap of the solution-phase line shape and the frequency bandwidth of the pump laser. From this study, we estimate that the C−H bend hot band is excited with about 40% efficiency (compared to resonance excitation). This factor, coupled with the fact that the probe absorption frequency will also be 20 cm^{-1} off-resonance (40% detection efficiency) and the hot-band population is 10% of the ground state, indicates that the dynamics of the combination state contribute about 1.6% to the measured signal and are, therefore, negligible.

Appendix C: Gas-Phase Data Analysis

Three of the molecules in this study have vibrational state densities below the 10 states/cm^{-1} threshold for observing IVR in molecular-beam experiments.[4,7] The measurements for these three molecules are shown in Figure A6. All three of these molecules (propyne, propargyl fluoride, and propargyl chloride) show some population decay at room temperature. For propyne, we observed a small-amplitude signal decay with a time constant of about 32 ps followed by a long decay on a time scale of about 500 ps. The mean collision time for propyne is estimated to be about 200 ps under the experimental conditions. The second relaxation time scale in propyne is consistent with this result if the relaxation probability for each collision is about 0.5. Sample diffusion rates out of the active laser volume ($d =$

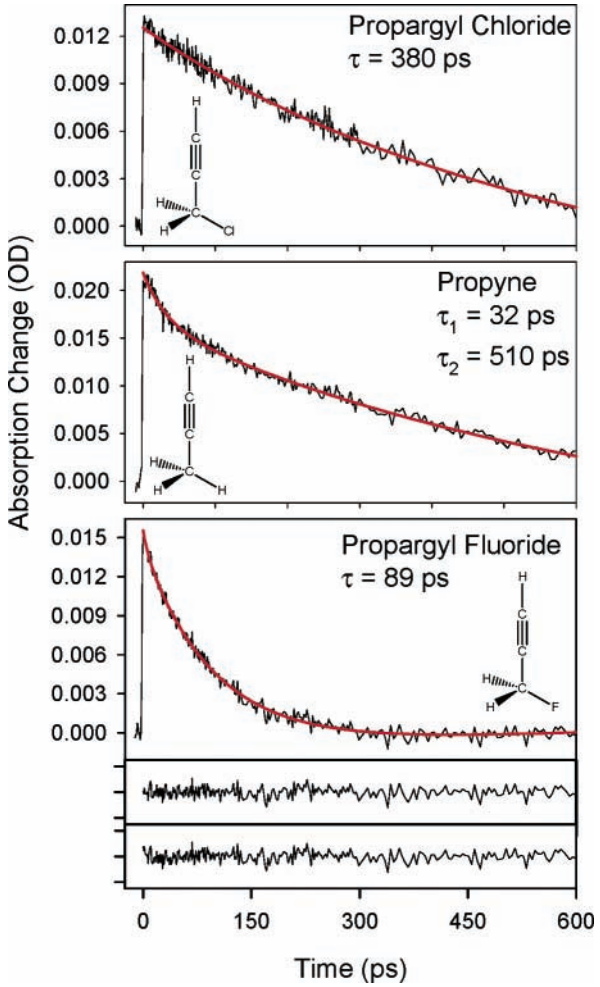

Figure A6. Transient absorption spectra of the first excited state of the acetylenic C−H stretch for three small molecules, which lie below the IVR threshold of ~10 states/cm^{-1}. The excited-state absorption of propargyl chloride decays on a very slow time scale (380 ps), whereas propyne and propargyl fluoride show a fast decay time scale. Propyne shows a small amplitude decrease during the fast decay process (32 ps), followed by a long decay (510 ps). Propargyl fluoride shows a full decay of the acetylenic C−H stretch excited-state population with a single time constant of 89 ps. Also, the residual plot to the single-exponential fit (lower residual) is shown along with the residual to the biexponential fit (upper residual) for propargyl fluoride. We attribute 32- and 89-ps decay times to the IVR lifetimes for propyne and propargyl fluoride, respectively.

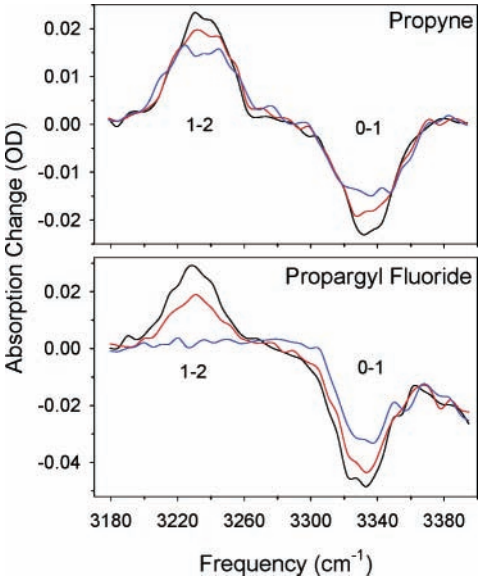

Figure A7. Transient absorption spectra of propyne and propargyl fluoride. The spectra are taken at three different time delays for both molecules: at $t = 0$, at $^1/_e$ time of the IVR decay, and at long time. The spectral range of these spectra covers the acetylenic C−H stretch fundamental and the anharmonically shifted $v = 1-v = 2$ absorption frequency. Propyne shows a unique inhomogeneous behavior, where the decay of the excited-state population is observed only in the central Q-branch region of the gas-phase spectrum, whereas propargyl fluoride shows a homogeneous decay of the whole rotational profile.

30 μm) are on the order of 100 ns for most of the molecules in this study and should not contribute to any of the decay signals. The transient absorption of the acetylenic C−H stretch excited state of propargyl fluoride decays to zero with a single, slower time constant (89 ps). This time scale appears to be too fast to attribute to collisional relaxation. Furthermore, we observe the same relaxation rate for propargyl fluoride when the experiment is performed at $^1/_5$ of the full vapor pressure. We attribute the 32-ps (propyne) and 89-ps (propargyl fluoride) decay times to IVR for these molecules.

We have further examined the vibrational relaxation of these two molecules by measuring the transient absorption spectrum at fixed time delay over a spectral range that covers the acetylenic C−H stretch fundamental and the anharmonically shifted excited-state absorption.[23,37,73,74] These spectra, shown in Figure A7, are measured at $t = 0$, the $^1/_e$ time of the IVR decay, and at long time. Propyne has a unique "inhomogeneous" behavior. The excited-state absorption and fundamental bleach recovery are observed only in the central Q-branch region of the gas-phase spectrum. In contrast, the full rotational band contour of propargyl fluoride changes at the same rate. The behavior of the propyne spectrum suggests that the IVR process is limited to states with high K rotational quantum numbers. (K is the projection of the total angular momentum, J, on the symmetric top axis.) The rotational selection rules for symmetric top molecules cause rotational levels with different values of K to dominate in Q and P/R branches.[75] For a given value of the total angular momentum, the rotational levels with $J = K$ are the strongest in the Q branch, and the levels with $K = 0$ are strongest in the P and R branches. Strongly K-dependent IVR rates, with the high K levels showing stronger interactions, have been observed in molecular-beam measurements of the propyne fundamental and overtones.[11−13]

The rotationally homogeneous change in the propargyl fluoride spectrum suggests that the measured rate is mainly due to anharmonic interactions. The observation of essentially complete population relaxation in propargyl fluoride was somewhat unexpected because of its low vibrational state density. However, higher-energy rotational levels (especially rotational levels with higher K_a values) of propargyl fluoride do show the near-resonant perturbations caused by IVR.[76] The fact that the whole rotational profile of propargyl fluoride decays at the same rate suggests that the rotational dependence of the IVR rate is small. All other molecules in this study show the same rotationally homogeneous spectral changes as propargyl fluoride, indicating that anharmonic interactions dominate rotationally mediated interactions (e.g., Coriolis interactions) in the IVR process even for the high-energy rotational levels. This conclusion is consistent with high-resolution molecular-beam infrared spectroscopy measurements that also show rotationally independent IVR rates.[4,8,10,52]

For propargyl chloride, a slow decay of the excited state on a 380-ps time scale is observed. This decay could be attributable either to IVR or collisional relaxation. IVR might be observable

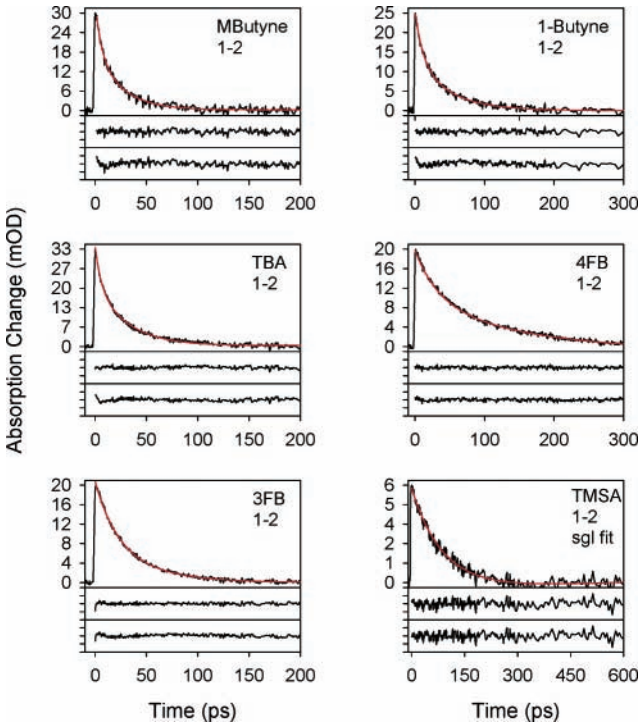

Figure A8. Decay of the excited-state population shown for larger molecules (vibrational state density of 10 states/cm^{-1} or greater at 3300 cm^{-1}). Except for TMSA, the excited-state population decays on two time scales, where a biexponential fit to each spectrum is shown as a red line. Residual plots of both the biexponential fit (upper residual plot) and single-exponential fit (lower residual plot) are shown.

in the room-temperature sample through rotationally induced interactions that would be more prevalent in the high-energy rotational levels that are now thermally populated. The relaxation rate is also consistent with an estimate of the mean collision time for propargyl chloride at the room-temperature vapor pressure (407 ps). However, on the basis of the propyne results we would not expect unit relaxation efficiency for each collision. In the data analysis, we assume that the propargyl chloride decay is caused by IVR. (However, because the measured rate is so slow, we obtain nearly identical results in all analyses if the IVR rate is set to zero).

Of the seven remaining molecules, only one (TMSA) has single-exponential decay of the excited-state population. For the rest of the molecules, the population relaxation occurs on multiple time scales. With the exception of methylbutenyne, these spectra can be fit using a simple biexponential decay expression (i.e., the sum of two independent exponentials). The time domain spectra of six terminal acetylenes are shown in Figure A8 along with biexponential decay fits to the spectra. The quality of both a single and a biexponential fit to the transient absorption spectrum is shown in the figure with residuals of each fit to the spectrum. These residual plots show the necessity for a biexponential fit (except for TMSA) to describe the decay of the excited-state population properly for large gas-phase molecules.

The time-dependent excited-state population of methylbutenyne has its own unique feature: a coherent oscillation with a period of about 2.8 ps. This measurement is shown in Figure A9. The coherent oscillation, which results from a strong anharmonic interaction with a single, nearly degenerate vibrational state, is damped with a time constant of about 4 ps. The identity of the perturbing vibrational state is considered in the next section of this paper. A second, longer time scale for the relaxation of about 23 ps is observed after the oscillation damps

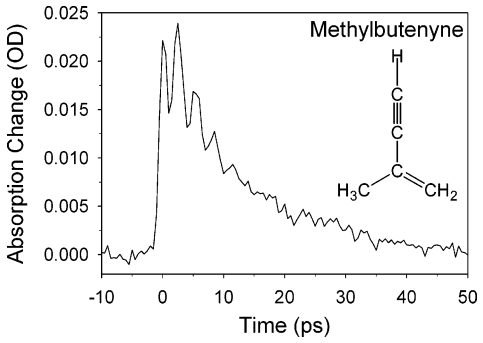

Figure A9. Time-dependent absorption signal change of the C−H stretch excited state for methylbutenyne. A coherent oscillation with a period of about 2.8 ps is observed. This coherent oscillation results from a strong anharmonic interaction with a single, nearly degenerate vibrational state. The oscillation is damped with two separate time constants of 4 and 23 ps. The fast time scale of 4 ps is the one that is comparable to the fast components of other molecules that show biexponential decay behavior and is the one that should be compared to the relaxation measurement of methylbutenyne in solution.

out. A complete analysis of the vibrational dynamics of methylbutenyne will be presented in a future publication.[72] This analysis indicates that the fast time scale that compares to the one observed in the other molecules in this study is the 4-ps damping time that measures the average IVR rate from the two strongly interacting vibrational states. Furthermore, this time scale is the one that should be compared to picosecond relaxation measurements of methylbutenyne in solution.

In the first application of picosecond infrared spectroscopy to gas-phase samples by Myers, Shigeiwa, Fayer, and Silbey, biexponential decay signals were also observed.[50] However, the fast component showed a pressure-dependent decay constant when argon was added to the sample. For this reason, the fast component was attributed to a process other than IVR, most likely spectral diffusion. Because the previous experiments used a single infrared frequency (i.e., a bleach-recovery measurement), the measured signals are sensitive to these effects. We measure the excited-state population directly through the anharmonically shifted $v = 1-v = 2$ transition of the acetylenic C−H stretch so that the biexponential signals can be definitively assigned to the IVR process. However, following the procedure in the previous work we have measured the gas-phase transient absorption spectra in the presence of high-pressure argon. The two time scales found in the pure gas are preserved when high-pressure inert gas is added, as shown for butyne in Figure A10.

Possible Origins of Biexponential Population Relaxation. The population relaxation of the acetylenic C−H stretch excited state occurs on two distinct time scales for several of the terminal acetylenes in this study. Two possible explanations for this behavior are considered in this section: (1) two different decay rates for separate populations in the inhomogeneous thermal sample and (2) a hierarchical IVR process for all thermally populated levels. The spectroscopic evidence favors the latter explanation for the observed gas-phase population decay signals.

1. Thermal Population Origin for the Biexponential Decay. We considered this possibility because of a similarity in the amplitudes of the two decay processes to the thermal population of the acetylenic wag normal-mode vibrations (i.e., the R−C≡C bending motion). The frequencies of the two wag normal modes depend on the R-group substituent because of mass effects in the kinetic energy but have a typical frequency of 200−300 cm^{-1} for the molecules in this study. Because there are two fundamentals of this type, the relative population of vibrational states with $v = 1$ and 0 in these modes is about 1:2

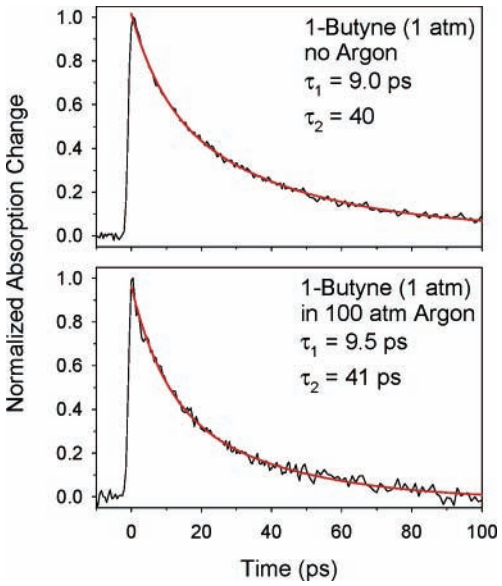

Figure A10. Pressure dependence of the excited-state population decay for butyne. The top panel shows the regular experimental conditions (1 atm of butyne in the sample cell), and the bottom panel is the measurement in the presence of an inert gas (1 atm of butyne in 100 atm of argon in the cell). The two time constants found in the pure gas are conserved when a high-pressure inert gas is added. However, as the total pressure in the cell increases, the relative amplitude of the fast component becomes larger: $A_1 = 0.37$ and $A_2 = 0.63$ for the pure butyne measurement; $A_1 = 0.49$ and $A_2 = 0.51$ for the measurement in the presence of 100 atm of argon.

at room temperature. This value is close to the ratio of the fast and slow rates found for molecules with biexponential decay of the acetylenic C−H stretch excited state (Table 2). In this model, the initial vibrational excitation of the acetylenic wag gets carried into the excited state by broadband excitation. These two populations would then have different IVR dynamics with excitation in the wag enhancing the IVR rate. The populations in other vibrational modes would have little influence on the IVR rate so that all thermally populated states could be grouped on the basis of the level of wag excitation. Vibrational states with 2 total quanta of wag excitation have only $^1/_5$ the population of the ground state. The contribution to the signal from these vibrational states might not be detectable with the current sensitivity (especially if the rate enhancement continues, making the IVR decay faster than the time resolution of the measurement).

In this model, the single-exponential solution rate would arise from fast, solvent-induced energy exchange between $v = 0$ and 1 of the wag. This rapid exchange would lead to the observation of a single, average decay rate in solution. A fast exchange is reasonable because the low-frequency vibrational mode can be expected to interact strongly with the solvent.[26,28,30,63,64,77] Efficient energy transfer in this mode is also supported by molecular-beam experiments, where we find that this mode is completely cooled in the expansion (whereas the acetylenic C−H bend, for example, maintains almost all of its initial thermal population). Because several solution rate measurements have decay times of less than 10 ps, the solvent exchange in the wag mode would have to be ∼1−5 ps to average the decay profile. One implication of fast energy exchange in this mode is that motional narrowing would be observed in any sequence band structure generated by the wag.[78−82] This effect is analogous to the collapse of nuclear hyperfine structure in NMR spectroscopy.[83] An exchange time of 1 ps would cause a collapse

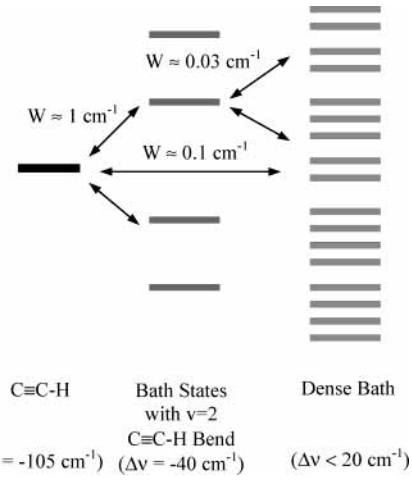

Figure A11. Tier model for the vibrational-energy relaxation process of the first excited state of the acetylenic C−H stretch. In this model, the acetylenic C−H stretch is strongly coupled to a sparse tier of vibrational states, which are assumed to have 2 quanta of the acetylenic C−H bend excitation. The acetylenic C−H stretch and the first tier are further coupled to a dense set of vibrational states. The vibrational states in the second tier are assumed to have either 1 or no quanta in the acetylenic C−H bend and represent the full state density of the molecule in the energy region of the acetylenic C−H stretch. Other parameters used in the calculations are the total energy range, 25 cm^{-1}; the number of first-tier states, 19 ($D_1 = 0.76$ states/cm^{-1}); and the number of second-tier states, 2000 ($D_2 = 80$ states/cm^{-1}).

of the sequence band when the frequency separation between adjacent transitions is less than ∼5 cm^{-1} ($\tau\Delta\omega \approx 1$).

The acetylenic wag has an observable off-diagonal anharmonicity with the acetylenic C≡C stretch. The gas-phase sequence band structure for propyne and propargyl fluoride caused by thermal population of the wag is shown in Figure A2. The frequency separation between adjacent hot-band Q branches is 7.7 and 4.3 cm^{-1} in propyne and propargyl fluoride, respectively. Coalescence of the sequence band structure would be expected in both molecules for a 1-ps (or faster) exchange time. However, the inhomogeneous structure persists in dilute solutions, as shown by the spectra in dilute CCl_4 solution also displayed in Figure A2. This model also fails to explain why two of the molecules that display gas-phase IVR (propargyl fluoride and TMSA) have decays that are well described by a single time constant. Although this model has some of the right features, it cannot explain the full data set of the terminal acetylenes.

2. Tier-Model Mechanism for IVR in Terminal Acetylenes. Vibrational dynamics of polyatomic molecules often occur on several distinct time scales. The most common example of IVR on distinct time scales occurs for molecules where the C−H stretch is near-resonant with the overtone of the C−H bend.[20,21,59,84−87] A particularly vivid example of IVR dynamics on separate time scales caused by stretch−bend interactions is benzene. The dynamics of this molecule are the subject of several experimental and theoretical studies.[88−92] Therefore, a possible interpretation of the picosecond measurements on the terminal acetylenes is that there is a well-defined hierarchy of anharmonic interactions of the C−H stretch with the vibrational bath.[69,70,93,94]

The dynamics and frequency-domain spectrum expected for a tier-model process are simulated by a random matrix calculation. The model used in this calculation is illustrated in Figure A11. The acetylenic C−H stretch is strongly coupled to a sparse tier of vibrational states. As indicated in the figure, the vibrational states in this tier are assumed to have 2 quanta of

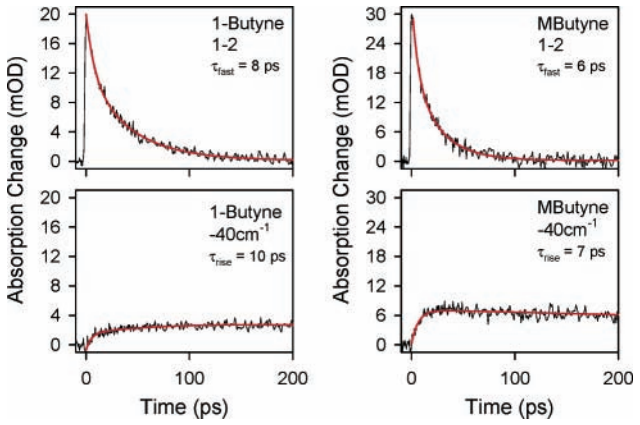

Figure A12. Time-domain spectra of butyne and methylbutyne. The excited-state population decays biexponentially (probing $\upsilon = 1-2$). On the time scale of the initial relaxation, we observe the population rise of vibrational states that include the overtone of the acetylenic C−H bend excited (probing −40 cm^{-1} from the fundamental frequency of the acetylenic C−H stretch).

the acetylenic C−H bend. This assignment is supported by the experiments as shown in Figure A12, where the population rise of the vibrational states with the overtone of the acetylenic C−H bend excitation is observed during the relaxation process. Because of the anharmonic interaction between the acetylenic C−H stretch and the acetylenic C−H bend as explained in Appendix A, the fundamental frequency of the acetylenic C−H stretch shifts about −40 cm^{-1} when the overtone of the acetylenic C−H bend is excited. Therefore, the population change of vibrational states with 2 quanta in the acetylenic C−H bend can be monitored at a frequency of −40 cm^{-1} from the acetylenic C−H stretch fundamental, as shown in Figure A12. This tier model is similar to the common stretch−bend interaction of other C−H stretches. However, in the terminal acetylenes the frequency of the C−H bend is much lower than for other C−H stretches (∼630 cm^{-1} fundamental frequency). Therefore, the direct stretch−bend interaction with the first overtone is well off-resonance. However, the energy gap of ∼2000 cm^{-1} between the C−H stretch and C−H bend overtone can be "closed" by excitation in other low-frequency normal modes.

There is one special case of this behavior for the terminal acetylenes: the energy gap is almost exactly equal to the frequency of the C≡C stretch. A relatively large anharmonic matrix element exists for the coupling between the C−H stretch and the combination band of the C≡C stretch and the C−H bend overtone ($W \approx 5-7$ cm^{-1}), and the resulting perturbation is a common feature in the vibrational spectrum of the terminal acetylenes.[11,66,67] For most of the molecules in the present study, this special resonance is unimportant to the vibrational dynamics because the combination band is 30−50 cm^{-1} higher in energy than the C−H stretch excited state. This interaction produces a weak perturbation that is observed in the FTIR spectrum, but this state lies outside the excitation bandwidth of the picosecond laser. However, for methylbutenyne the combination state is brought into resonance through the frequency lowering of the out-of-plane bend that is caused by conjugation with the C=C bond.[57] The strong interaction with this single, first-tier state ($W \approx 6$ cm^{-1}) produces the fast coherent oscillation in Figure A9.[72] For the other molecules, the important interactions involve vibrational states where the energy gap is made up of 2 or more vibrational quanta in other vibrational modes. This set of vibrational bath states is sparse because so much of the total energy is localized in a single vibrational mode (the C−H bend).

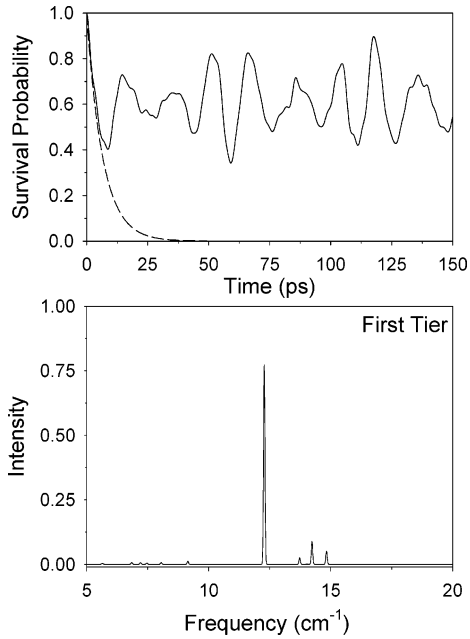

Figure A13. Survival probability of the C−H stretch excited state shown for the tier model of Figure A11. This result is obtained with a reduced model calculation, where only the first tier is included in the survival probability calculation. The initial relaxation is followed by a population oscillation around the dilution factor (ϕ_d). The initial decay rate is estimated using the Fermi Golden Rule rate and is indicated as a dashed line. The vibrational spectrum from the reduced model calculation (bottom panel) shows the lack of extensive local perturbations.

The bend overtone tier and the acetylenic C−H stretch itself are then coupled to a dense set of vibrational states with either 1 or no quanta in the C−H bend. This tier has essentially the full state density of the molecule at the energy of the C−H stretch. The choice of root-mean-squared matrix elements for coupling to the second tier is motivated by an analysis of the molecular-beam spectra of methylbutenyne and will be discussed in a future publication.[72]

The random matrix calculation is performed in two steps. In the first step, the vibrational dynamics and spectrum are calculated without the second tier of states. The results of this reduced model are then compared to the full calculation. The results of a representative calculation are shown to illustrate the main behavior expected from the model. The reduced model (first-tier only) falls in the sparse limit of IVR. (This limit is characterized by the relation $\rho W < 1$, where ρ is the density of first-tier states and W is the root-mean-squared (rms) interaction matrix element.[95]) The population of the C−H stretch excited state for the reduced model is calculated through the survival probability[96] and shown in Figure A13. There is an initial decay of the population followed by a highly structured "quantum beat" pattern. The initial decay rate can be approximated using the Fermi Golden Rule rate

$$\Gamma = 2\pi\langle W^2\rangle\rho \qquad \text{(A1)}$$

and the initial decay rate to the first tier is shown in Figure A13 as a single-exponential decay. At longer time, the excited-state population oscillates around an average value given by the incoherent contribution to the survival probability, called the dilution factor (ϕ_d). This average value can be used to define an effective number of coupled states (N_{eff}). The definition of these terms will be presented in detail in the following paper.[96] The number of effectively coupled states (N_{eff}) is much lower

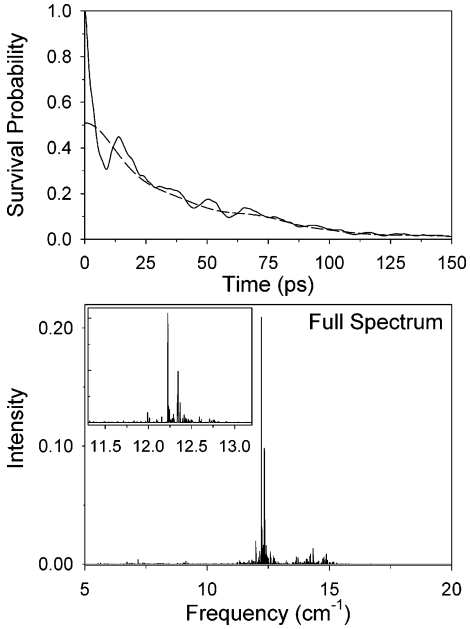

Figure A14. Survival probability calculation of the full tier model is shown in the top panel. The relaxation of the excited-state population is biexponential. The initial decay shows the time scale of the energy flow from the excited state to the first tier, and the time scale of the energy flow into the dense bath is reflected by the slow component. The vibrational spectrum of the full tier model calculation is shown in the bottom panel. The further fragmentation from the reduced model calculation (Figure A13) is observed because of the coupling to the dense second tier. The central main feature is shown in the inset. The survival probability calculation using this main feature only is also shown in the top panel as a dashed line, which is shown to control the second, slower time scale of the vibrational dynamics.

than the actual number of first-tier states coupled to the bright state. The vibrational spectrum from this reduced model is also shown in Figure A13 and is dominated by a single feature.[69,70] The wave function of this feature contains contributions from the acetylenic C−H stretch and the coupled first-tier states.

In the presence of the dense second tier, the population dynamics of the excited state include an overall decay that reflects the time scale of energy flow into the dense bath, producing an approximate biexponential decay of the excited-state population (Figure A14). The spectrum when the second tier is included is also shown in Figure A14. The main effect of the coupling to the second tier is the further fragmentation of each spectral feature of the reduced model. A single absorption feature dominates the full model spectrum. The survival probability calculated from the spectrum of the main feature is also shown in Figure A14. The second, slower time scale of the vibrational dynamics is controlled by this part of the full spectrum, which will be shown to be related to the molecular-beam IVR rates in the third paper of this series.[96]

With the tier-model explanation of the gas-phase picosecond vibrational dynamics, the fast component of the decay is related to the relaxation rate in solution. We propose that the IVR contribution to the solution-phase relaxation rate is governed by the initial IVR rate of the C−H stretch (i.e., the fast component measured in the gas phase). The observation of a biexponential decay process is related to the fact that the vibrational dynamics of the first tier lead to restricted IVR. The relatively low amplitude of the initial decay in the gas phase is caused by coherent energy flow that allows the energy to return to the acetylenic C−H stretch from the first-tier states. To observe this behavior, it is crucial that the phase relationships between the coupled states are maintained. If the relative phase

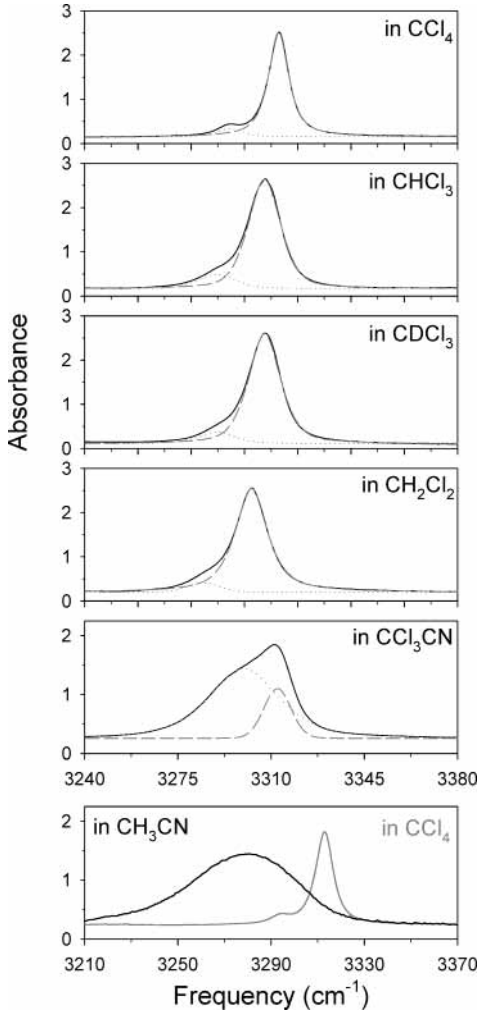

Figure A15. FTIR spectra of propargyl chloride in five solvents shown for the acetylenic C−H stretch fundamental frequency region. In general, the line width and the spectral shift increase with solvent polarity. The line-shape changes are analyzed using a pseudo-Voigt profile, where the relative contribution of the Lorentzian and Gaussian contributions can be varied (Table A1). In the bottom panel, scaled line shapes of propargyl chloride in CH_3CN and CCl_4 are shown together to compare to the unusual line shape in CCl_3CN.

can be interrupted, then the dynamics follow incoherent dynamics[97−100] and the population will decay to the reciprocal of the number of states participating in the dynamics, not the lower coherent value of N_{eff}. In solution, the phase information can be destroyed through the pure dephasing process (T_2*), which damps the coherent intramolecular oscillations.[101] In a future paper, we will describe this model in detail and show how it affects the population decay of coherently excited two-level systems (such as methylbutenyne) in solution.[102]

Appendix D: Solution-Phase Line Shapes of the Acetylenic C−H Stretch Absorption Spectrum

In this section, we examine the solution-phase line shapes of the acetylenic C−H stretch absorption spectrum in different solvents. The FTIR spectra of propargyl chloride in the five solvents we have investigated are shown in Figure A15. The spectra of the other terminal acetylenes in these solvents are virtually identical (except for methylbutenyne, where the resonant perturbation with the C≡C stretch + 2C−H bend combination state causes an additional broadening). The line shapes are simple for all solvents except CCl_3CN. A likely

TABLE A1: Spectral Parameters of Propargyl Chloride for the Acetylenic C−H Stretch in Five Solvents

solvent	center frequency (cm^{-1})	fwhm (cm^{-1})	fraction of Lorentzian character	solvent dipole moment
CCl_4	3313	8.5	0.79	0
$CHCl_3$	3308	12.3	0.51	1.0
$CDCl_3$	3308	12.5	0.63	1.0
CH_2Cl_2	3303	13.3	0.77	1.6
CCl_3CN	3312	10.2	0.53	2.0

explanation for the line shape in CCl_3CN is that the terminal acetylenes are found in two microscopic environments: the acetylenic C−H stretch solvated by the $-CCl_3$ end of the molecule or by the $-C\equiv N$ end of the solvent. This possibility is supported by comparing the acetylenic C−H stretch spectrum in dilute CCl_4 and CH_3CN solutions (shown in the bottom panel of Figure A15). In our measurements, we excite at the peak of the solution line shape, which would be assigned to solvation by the $-CCl_3$ end of the solvent in this interpretation. Despite the possibility of solvent reorganization dynamics occurring,[103] we observe no anomalous behavior in the rate measurements for this solvent.

In general, the line width and shift of the spectrum increase with solvent polarity. The line shape also changes, becoming more Gaussian in shape as the solvent polarity is increased. We have quantified the line-shape changes by fitting the spectra to a pseudo-Voigt profile.[104] This line shape uses a single width parameter but permits the relative contributions of the Lorentzian and Gaussian contributions to vary. The fractional "Lorentzian character" is reported in Table A1 with other basic spectral properties. These changes in line shape indicate that the spectrum lies further from the motional narrowing regime with increasing polarity.[105]

References and Notes

(1) Nesbitt, D. J.; Field, R. W. *J. Phys. Chem.* **1996**, *100*, 12735.
(2) Baer, T.; Hase, W. L. *Unimolecular Reaction Dynamics*; Oxford University Press: New York, 1996.
(3) Quack, M. *Annu. Rev. Phys. Chem.* **1990**, *41*, 839.
(4) Lehmann, K. K.; Scoles, G.; Pate, B. H. *Annu. Rev. Phys. Chem.* **1994**, *45*, 241.
(5) Voth, G. A.; Hochstrasser, R. M. *J. Phys. Chem. A* **1996**, *100*, 13034.
(6) Owrutsky, J. C.; Raftery, D.; Hochstrasser, R. M. *Annu. Rev. Phys. Chem.* **1994**, *45*, 519.
(7) Kim, H. L.; Kulp, T. J.; McDonald, J. D. *J. Chem. Phys.* **1987**, *87*, 4376.
(8) de Souza, A. M.; Kaur, D.; Perry, D. S. *J. Chem. Phys.* **1988**, *88*, 4569.
(9) McIlroy, A.; Nesbitt, D. J. *J. Chem. Phys.* **1989**, *91*, 104.
(10) McIlroy, A.; Nesbitt, D. J. *J. Chem. Phys.* **1990**, *92*, 2229.
(11) Kerstel, E. R. Th.; Lehmann, K. K.; Pate, B. H.; Scoles, G. *J. Chem. Phys.* **1994**, *100*, 2588.
(12) McIloy, A.; Nesbitt, D. J.; Kerstel, E. R. T.; Pate, B. H.; Lehmann, K. K.; Scoles, G. *J. Chem. Phys.* **1994**, *100*, 2596.
(13) Gambogi, J. E.; Kerstel, E. R. Th.; Lehmann, K. K.; Scoles, G. *J. Chem. Phys.* **1994**, *100*, 2612.
(14) Green, D.; Hammond, S.; Keske, J.; Pate, B. H. *J. Chem. Phys.* **1999**, *110*, 1979.
(15) Li, H.; Miller, C. C.; Philips, L. A. *J. Chem. Phys.* **1994**, *100*, 8590.
(16) Kenkre, V. M.; Tokmakoff, A.; Fayer, M. D. *J. Chem. Phys.* **1994**, *101*, 10618.
(17) Deàk, J. C.; Iwaki, L. K.; Dlott, D. D. *J. Phys. Chem. A* **1999**, *103*, 971.
(18) Iwaki, L. K.; Dlott, D. D. *Chem. Phys. Lett.* **2000**, *321*, 419.
(19) Hofmann, M.; Graener, H. *Chem. Phys.* **1996**, *206*, 129.
(20) Graener, H.; Zürl, R.; Hofmann, M. *J. Phys. Chem. B* **1997**, *101*, 1745.
(21) Bakker, H. J.; Planken, P. C. M.; Kuipers, L.; Lagendijk, A. *J. Chem. Phys.* **1991**, *94*, 1730.
(22) Bakker, H. J.; Planken, P. C. M.; Lagendijk, A. *J. Chem. Phys.* **1991**, *94*, 6007.
(23) Bonn, M.; Brugmans, M. J. P.; Bakker, H. J. *Chem. Phys. Lett.* **1996**, *249*, 81.
(24) Bakker, H. J. *J. Chem. Phys.* **1993**, *98*, 8496.
(25) Zinth, W.; Kolmeder, C.; Benna, B.; Irgens-Defregger, A.; Fischer, S. F.; Kaiser, W. *J. Chem. Phys.* **1983**, *78*, 3916.
(26) Bagchi, B.; Oxtoby, D. W. *J. Chem. Phys.* **1983**, *78*, 2735.
(27) Stratt, R. M.; Maroncelli, M. *J. Phys. Chem.* **1996**, *100*, 12981.
(28) Rey, R.; Hynes, J. T. *J. Chem. Phys.* **1996**, *104*, 2356.
(29) Egorov, S. A.; Skinner, J. L. *J. Chem. Phys.* **2000**, *112*, 275.
(30) Sibert, E. L.; Rey, R. *J. Chem. Phys.* **2002**, *116*, 237.
(31) Heilweil, E. J.; Casassa, M. P.; Cavanagh, R. R.; Stephenson, J. C. *J. Chem. Phys.* **1986**, *85*, 5004.
(32) Fraser, G. T.; Pate, B. H.; Bethardy, G. A.; Perry, D. S. *Chem. Phys.* **1993**, *175*, 223.
(33) Laenen, R.; Rauscher, C. *Chem. Phys. Lett.* **1997**, *274*, 63.
(34) Hudspeth, E.; McWhorter, D. A.; Pate, B. H. *J. Chem. Phys.* **1998**, *109*, 4316.
(35) Self-Medlin, Y. B.; Yoo, H. S.; Pate, B. H. Unpublished data.
(36) Ebata, T.; Kayano, M.; Sato, S.; Mikami, N. *J. Phys. Chem. A* **2001**, *105*, 8623.
(37) Laenen, R.; Simeonidis, K. *Chem. Phys. Lett.* **1999**, *299*, 589.
(38) Aubuchon, C. M.; Rector, K. D.; Holmes, W.; Fayer, M. D. *Chem. Phys. Lett.* **1999**, *299*, 84.
(39) Assmann, J.; Charvat, A.; Schwarzer, D.; Kappel, C.; Luther, K.; Abel, B. *J. Phys. Chem. A* **2002**, *106*, 5197.
(40) Assmann, J.; Benten, R. v.; Charvat, A.; Abel, B. *J. Phys. Chem. A* **2003**, *107*, 1904.
(41) Assmann, J.; Benten, R. v.; Charvat, A.; Abel, B. *J. Phys. Chem. A* **2003**, *107*, 5291.
(42) Bingemann, D.; King, A. M.; Crim, F. F. *J. Chem. Phys.* **2000**, *113*, 5018.
(43) Cheatum, C. M.; Heckscher, M. M.; Bingemann, D.; Crim, F. F. *J. Chem. Phys.* **2001**, *115*, 7086.
(44) Heckscher, M. M.; Sheps, L.; Bingemann, D.; Crim, F. F. *J. Chem. Phys.* **2002**, *117*, 8917.
(45) Elles, C. G.; Bingemann, D.; Heckscher, M. M.; Crim, F. F. *J. Chem. Phys.* **2003**, *118*, 5587.
(46) Charvat, A.; Assmann, J.; Abel, B.; Schwarzer, D. *J. Phys. Chem. A* **2001**, *105*, 5071.
(47) Sekiguchi, K.; Shimojima, A.; Kajimoto, O. *Chem. Phys. Lett.* **2002**, *356*, 84.
(48) Urdahl, R. S.; Rector, K. D.; Myers, D. J.; Davis, P. H.; Fayer, M. D. *J. Chem. Phys.* **1996**, *105*, 8973.
(49) Urdahl, R. S.; Myers, D. J.; Rector, K. D.; Davis, P. H.; Cherayil, B. J.; Fayer, M. D. *J. Chem. Phys.* **1997**, *107*, 3747.
(50) Myers, D. J.; Shigeiwa, M.; Fayer, M. D.; Silbey, R. *Chem. Phys. Lett.* **1999**, *312*, 399.
(51) Woutersen, S.; Emmerichs, U.; Bakker, H. J. *J. Chem. Phys.* **1997**, *107*, 1483.
(52) Engelhardt, C.; Keske, J. C.; Rees, F. S.; Self-Medlin, Y. B.; Yoo, H. S.; Pate, B. H. *J. Phys. Chem. A* **2001**, *105*, 6800.
(53) Kraihanzel, C. S.; West, R. *J. Am. Chem. Soc.* **1962**, *84*, 3670.
(54) Dübal, H. R.; Quack, M. *Chem. Phys. Lett.* **1982**, *90*, 370.
(55) Quack, M. *Jerusalem Symp. Quantum Chem. Biochem.* **1991**, *24*, 47.
(56) Jona, P.; Gussoni, M.; Zerbi, G. *J. Phys. Chem.* **1981**, *85*, 2210.
(57) Nyquist, R. A.; Potts, W. J. *Spectrochim. Acta* **1960**, *16*, 419.
(58) Evans, J. C.; Nyquist, R. A. *Spectrochm. Acta* **1963**, *19*, 1153.
(59) Kolmeder, C.; Zinth, W.; Kaiser, W. *Chem. Phys. Lett.* **1982**, *91*, 323.
(60) Murchison, C. B.; Overend, J. *Spectrochim. Acta, Part A* **1971**, *27*, 1509.
(61) Smith, D. F.; Overend, J. *Spectrochim. Acta, Part A* **1972**, *28*, 87.
(62) Velsko, S.; Oxtoby, D. W. *J. Chem. Phys.* **1980**, *72*, 2260.
(63) Grote, R. F.; van der Zwan, G.; Hynes, J. T. *J. Phys. Chem.* **1984**, *88*, 4676.
(64) Egorov, S. A.; Skinner, J. L. *J. Chem. Phys.* **1996**, *105*, 7047.
(65) Stratt, R. M. *Acc. Chem. Res.* **1995**, *28*, 201.
(66) Duncan, J. L.; McKean, D. C.; Nivellini, G. D. *J. Mol. Struct.* **1976**, *32*, 255.
(67) Lafferty, W. J.; Pine, A. S. *J. Mol. Spectrosc.* **1990**, *141*, 223.
(68) Keske, J. C.; Rees, F. S.; Pate, B. H. Unpublished data.
(69) Stuchebrukhov, A. A.; Marcus, R. A. *J. Chem. Phys.* **1993**, *98*, 6044.
(70) Stuchebrukhov, A. A.; Mehta, A.; Marcus, R. A. *J. Phys. Chem.* **1993**, *97*, 12491.
(71) The vibrational frequencies were calculated at the B3LYP/6−31 g** level using the Gaussian 98 program. Frisch, M. J.; Trucks, G. W.; Schlegel, H. B.; Scuseria, G. E.; Robb, M. A.; Cheeseman, J. R.; Zakrzewski, V. G.; Montgomery, J. A., Jr.; Stratmann, R. E.; Burant, J. C.; Dapprich, S.; Millam, J. M.; Daniels, A. D.; Kudin, K. N.; Strain, M. C.; Farkas, O.; Tomasi, J.; Barone, V.; Cossi, M.; Cammi, R.; Mennucci, B.; Pomelli, C.;

Adamo, C.; Clifford, S.; Ochterski, J.; Petersson, G. A.; Ayala, P. Y.; Cui, Q.; Morokuma, K.; Malick, D. K.; Rabuck, A. D.; Raghavachari, K.; Foresman, J. B.; Cioslowski, J.; Ortiz, J. V.; Stefanov, B. B.; Liu, G.; Liashenko, A.; Piskorz, P.; Komaromi, I.; Gomperts, R.; Martin, R. L.; Fox, D. J.; Keith, T.; Al-Laham, M. A.; Peng, C. Y.; Nanayakkara, A.; Gonzalez, C.; Challacombe, M.; Gill, P. M. W.; Johnson, B. G.; Chen, W.; Wong, M. W.; Andres, J. L.; Head-Gordon, M.; Replogle, E. S.; Pople, J. A. *Gaussian 98W*, version 5.2; Gaussian, Inc.: Pittsburgh, PA, 1998.

(72) Yoo, H. S.; Rees, F. S.; Brown, G.; Douglass, K. O.; Johns, J.; Keske, J. C.; Nair, P.; Pate, B. H. Submitted.

(73) Dougherty, T. P.; Heilweil, E. J. *Opt. Lett.* **1994**, *19*, 129.

(74) Arrivo, S. M.; Dougherty, T. P.; Grubbs, W. T.; Heilweil, E. J. *Chem. Phys. Lett.* **1995**, *235*, 247.

(75) Papoušek, D.; Aliev, M. R. *Molecular Vibrational−Rotational Spectra*; Elsevier: New York, 1982.

(76) Rees, F. S.; Pate, B. H. Unpublished data.

(77) Deng, Y.; Stratt, R. M. *J. Chem. Phys.* **2002**, *117*, 1735.

(78) Harris, C. B.; Shelby, R. M.; Cornelius, P. A. *Chem. Phys. Lett.* **1978**, *57*, 8.

(79) Shelby, R. M.; Harris, C. B.; Cornelius, P. A. *J. Chem. Phys.* **1979**, *70*, 34.

(80) Wertheimer, R. K. *Mol. Phys.* **1978**, *35*, 257.

(81) Wertheimer, R. K. *Mol. Phys.* **1979**, *38*, 797.

(82) Wertheimer, R. K. *Chem. Phys.* **1980**, *45*, 415.

(83) Abragam, A. *Principles of Nuclear Magnetics*; Oxford University Press: New York, 1996.

(84) Segall, J.; Zare, R. N.; Dübal, H. R.; Lewerenz, M.; Quack, M. *J. Chem. Phys.* **1987**, *86*, 634.

(85) Pochert, J.; Quack, M. *Mol. Phys.* **1998**, *95*, 1055.

(86) Fendt, A.; Fischer, S. F.; Kaiser, W. *Chem. Phys.* **1981**, *57*, 55.

(87) Seifert, G.; Zürl, R.; Patzlaff, T.; Graener, H. *J. Chem. Phys.* **2000**, *112*, 6349.

(88) Sibert, E. L.; Reinhardt, W. P.; Hynes, J. T. *J. Chem. Phys.* **1984**, *81*, 1115.

(89) Scotoni, M.; Boschetti, A.; Oberhofer, N.; Bassi, D. *J. Chem. Phys.* **1991**, *94*, 971.

(90) Page, R. H.; Shen, Y. R.; Lee, Y. T. *J. Chem. Phys.* **1988**, *88*, 4621.

(91) Callegari, A.; Srivastava, H. K.; Merker, U.; Lehmann, K. K.; Scoles, G.; Davis, M. J. *J. Chem. Phys.* **1997**, *106*, 432.

(92) Callegari, A.; Merker, U.; Engels, P.; Srivastava, H. K.; Lehmann, K. K.; Scoles, G. *J. Chem. Phys.* **2000**, *113*, 10583.

(93) Quack, M.; Stohner, J. *J. Phys. Chem.* **1993**, *97*, 12574.

(94) Gruebele, M.; Bigwood, R. *Int. Rev. Phys. Chem.* **1998**, *17*, 91.

(95) Jortner, J.; Levine, R. D. *Adv. Chem. Phys.* **1981**, *47*, 1.

(96) Yoo, H. S.; McWhorter, D. A.; Pate, B. H. *J. Phys. Chem. A* **2004**, *108*, 1380.

(97) Kay, K. G.; Rice, S. A. *J. Chem. Phys.* **1972**, *57*, 3041.

(98) Heller, E. J.; Rice, S. A. *J. Chem. Phys.* **1974**, *61*, 936.

(99) Muthukumar, M.; Rice, S. A. *J. Chem. Phys.* **1978**, *69*, 1619.

(100) Shore, B. W. *The Theory of Coherent Atomic Excitation*; Wiley & Sons: New York, 1990; Vol. 2.

(101) Ungar, L. W.; Cina, J. A. *J. Phys. Chem. A* **1998**, *102*, 7382.

(102) Yoo, H. S.; DeWitt, M. J.; Pate, B. H. In preparation.

(103) Arrivo, S. M.; Heilweil, E. J. *J. Phys. Chem.* **1996**, *100*, 11975.

(104) pseudo-Voigt $= \text{amp}\cdot\left[f\cdot\left(\frac{1}{1+\left(x-x_0/\text{HWHM}\right)^2}\right)+(1-f)\cdot\exp\left(-0.5\cdot\left(\frac{x-x_0}{\text{HWHM}}\right)^2\right)\right]+c$.

(105) Oxtoby, D. W. *Annu. Rev. Phys. Chem.* **1981**, *32*, 77.